COLLÈGE DE FRANCE
1530

Chaire de Physique
de la Matière Condensée
Antoine Georges

Contrôle des fonctionnalités des oxydes

Hétéro-structures, Impulsions Lumineuses

Cours 6 – Contrôle par impulsions lumineuses, « Phononique non-linéaire »

Cycle 2016-2017
30 mai 2017

COLLÈGE DE FRANCE 1530

Chaire de Physique
de la Matière Condensée
Antoine Georges

Control of oxide functionalities:

Heterostructures,
Light pulses

Lecture 6 – Control by light pulses,

« Non-Linear Phononics »

Most slides will be in English

2016-2017 Lectures
May 30, 2017

Today’s seminar – May 30

Manuel Bibes

CNRS – Thales

Electric field control of magnetism in oxide heterostructures

http://oxitronics.wordpress.com

This is the last lecture of this 2016-2017 cycle

BUT:

On Tue June, 13 at 10:00

We shall have a seminar

by Olle Eriksson

University of Uppsala

Data-mining approaches to find new materials

In this presentation I will introduce electronic structure theory, and describe how information calculated without input from experiments (so called ab-initio theory) can be used to find materials with potentially tailored properties. Examples will be given for potentially new superconductors, new two-dimensional materials as well as correlated electronic structures where the Kondo effects sets in. I will also outline how theory can be used to make a connection to an effective spin-Hamiltonian, for investigations of magnetization dynamics at time-scales down to sub-pico-seconds, and examples of simulations of all-thermal switching will be given.

One more announcement:
Lectures on Novel Phenomena at Oxide Interfaces
by Jacobo Santamaria (Madrid)
at CNRS-Thales
June 6, 12, 19, 26

Dans le cadre du programme "Bourse Jean D'Alembert" de l'Université Paris-Saclay, le Professeur Jacobo Santamaria de Universidad Complutense Madrid, accueilli par l'Unité Mixte de Physique CNRS/Thales, donnera une série de cours en juin 2017. Ces cours sont validés par l'Ecole Doctorale PIF.

« Lectures on Novel Phenomena at Oxide Interfaces » (https://www.edpif.org/misc/2017/Lectures%20J.Santamaria_UPSay_June%202017%20.pdf) –

Prof. Jacobo Santamaria - Universidad Complutense Madrid Jacobo Santamaria

Dates : du mardi 06 juin 2017 au lundi 26 juin 2017

Lieux : Thales-RT entrance building

Inscr. : Envoyer un email à Javier Villegas (javier.villegas@cnrs-thales.fr (mailto:javier.villegas@cnrs-thales.fr))

- Lecture 1. Introduction to the physics of oxide interfaces

Tuesday June 6, 14:30-16:30, room 1C-50 (1st floor, Thales-RT entrance building)

- Lecture 2. Novel functionalities at oxide interfaces

Monday June 12, 14:30-16:30, room 2C-50 (2nd floor, Thales-RT entrance building)

- Lecture 3. Novel proximity phenomena at superconducting oxide interfaces

Monday June 19, 14:30-16:30, room 2C-50 (2nd floor, Thales-RT entrance building)

- Lecture 4. Nanoionics at oxide interfaces

Monday June 26, 14:30-16:30, room 2C-50 (2nd floor, Thales-RT entrance building)

SELECTIVE structural control

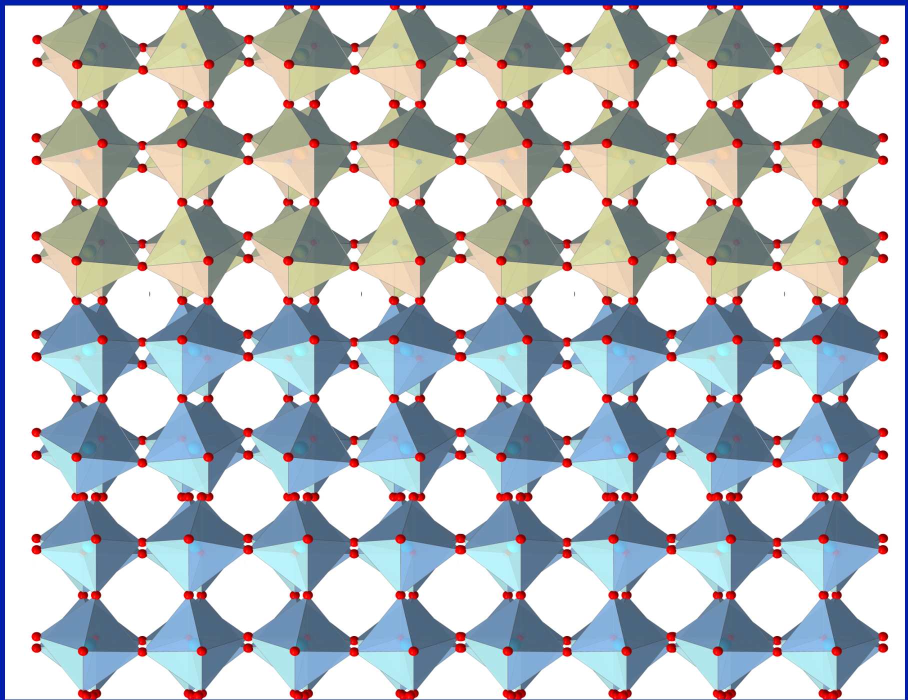

Artificial Materials
- Strained films and Heterostructures

Selective control with LIGHT

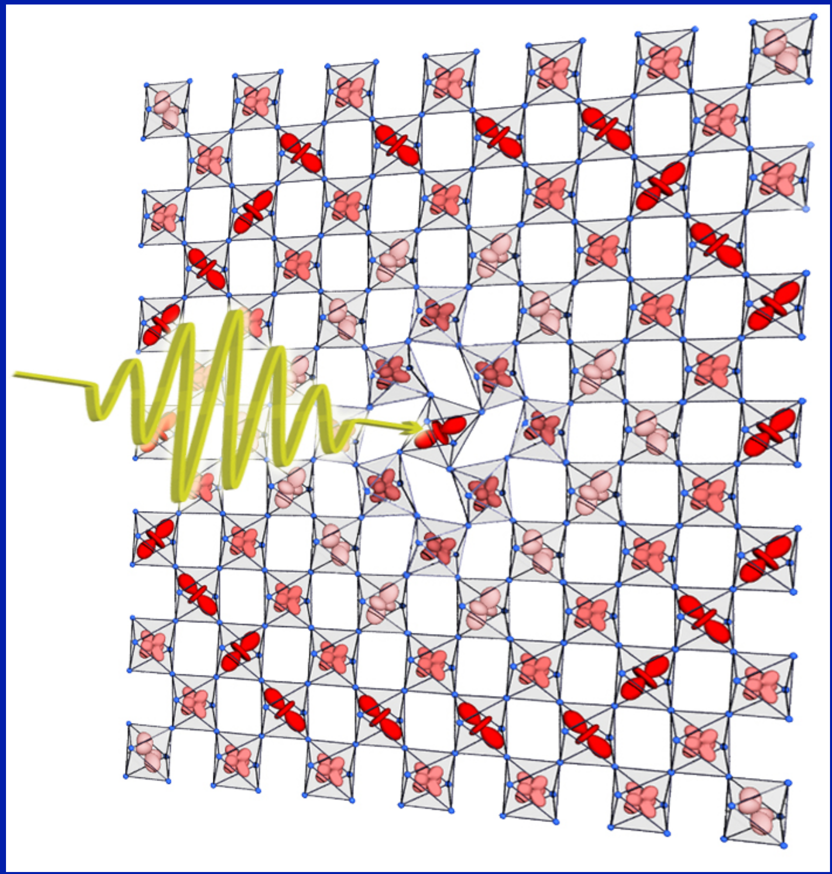

Structure determines Function

For example:

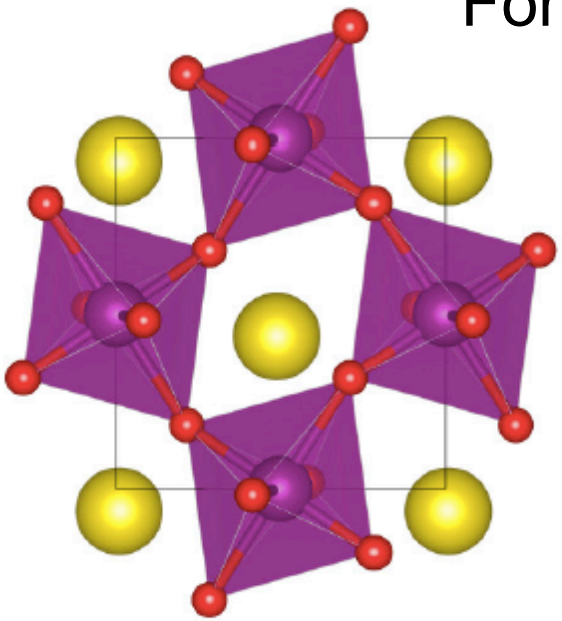

Large rotation/distortion
Insulating

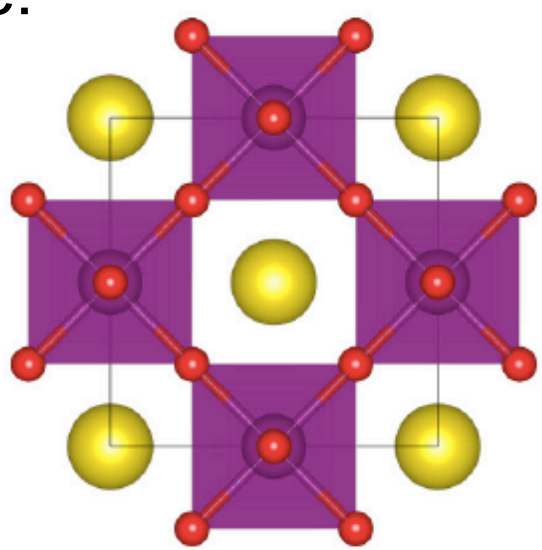

No rotation/distortion
Metallic
Undistorted phase not synthesized

Change of structure in turn changes key electronic energy scales
- such as: Bandwidth, Energy splitting between orbitals (xtal-field), superexchange, etc…

Selective control with resonant light

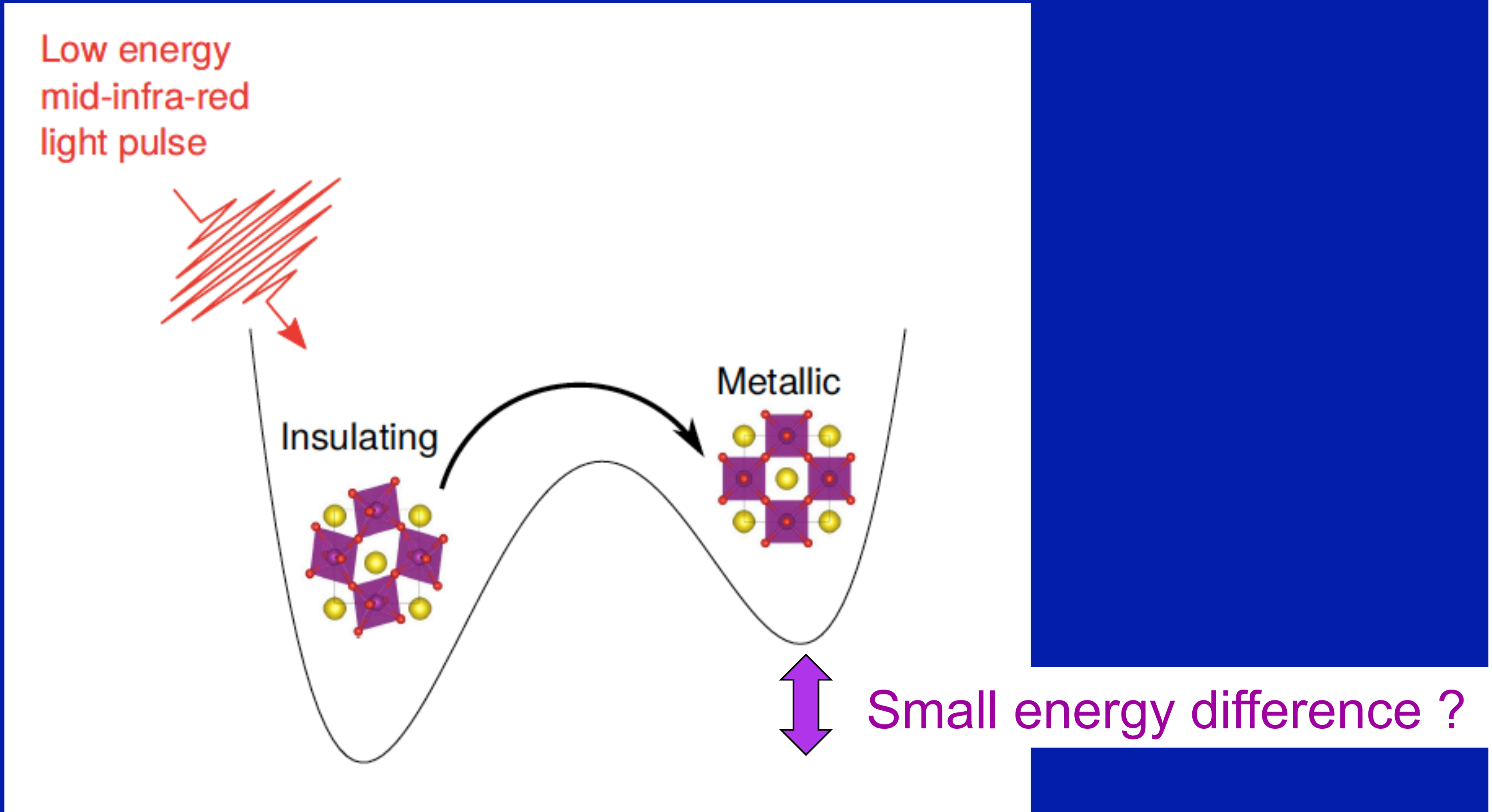

Create transient structures which cannot be synthesized at equilibrium !

CONTROLLING
electronic properties of correlated quantum materials
via SELECTIVE CONTROL of <u>structure</u>

“Frontiers in Quantum Materials Control”
ERC-Synergy project QMAC
A.Cavalleri, A.G., D.Jaksch, J.M. Triscone

http://www.mpsd.mpg.de/48916/Q-MAC-start

European Research Council

Part of a broader field: pump-probe spectroscopies

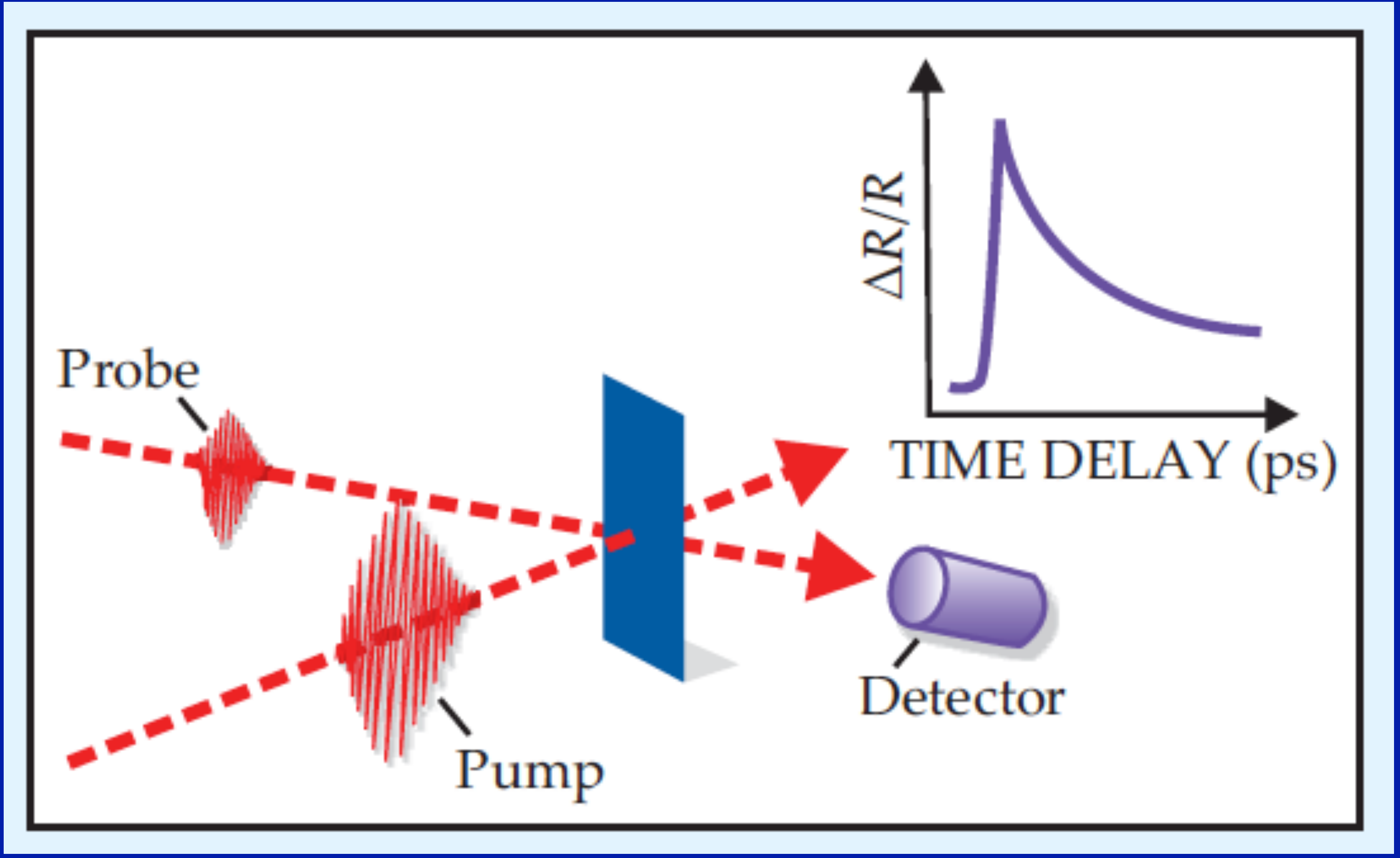

From: J.Orenstein, Physics Today, Sep 2012

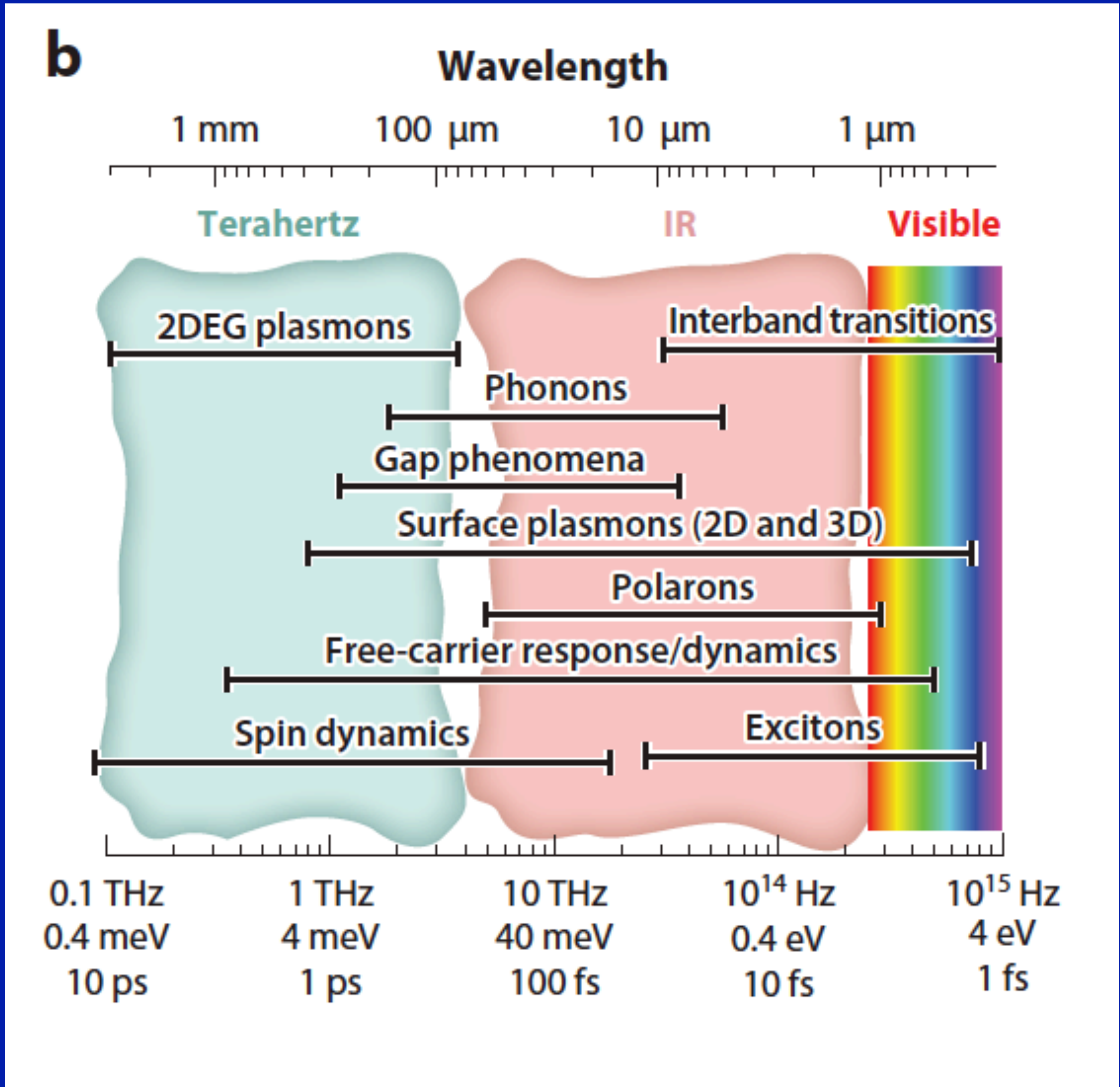

From Zhang and Averitt Ann Rev Mat Res 2014

Incoherent vs. Coherent Control

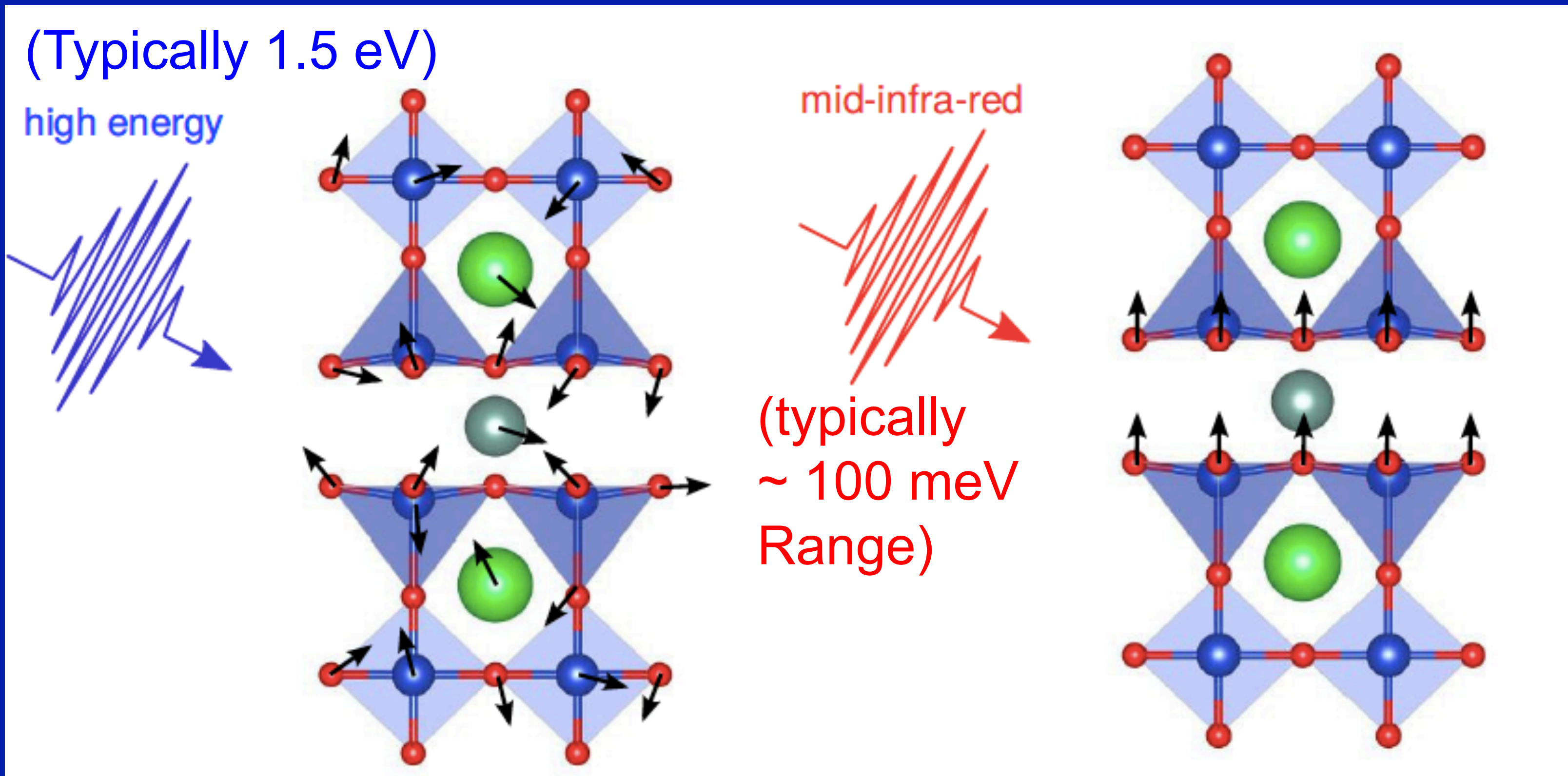

Incoherent excitation
heats the material
poorly selective

Coherent excitation
low dissipation due to heat
excites only a few degrees of
freedom

Mid-infrared pumps: Optical Parametric Amplification
+ Difference Frequency Generation cf. A.Cavalleri's lectures

Pioneering experiments by Andrea Cavalleri et al.

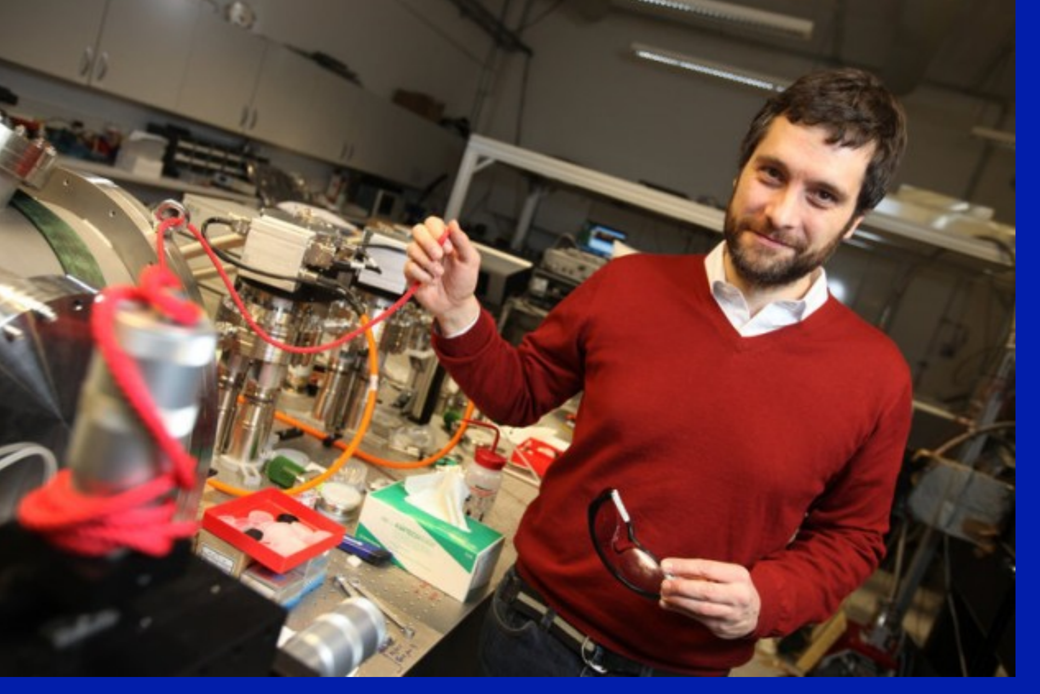

See lectures at the College de France, Feb 2017:
https://www.college-de-france.fr/site/antoine-georges/guestlecturer-2016-2017.htm

An early experiment: Metallization of a Manganite by selective excitation of mid-IR structural mode

Exciting an IR-active phonon
(up and down shaking of octahedra 71 meV ~ 17 THz)
in an insulating manganite *induces an Insulator-to-Metal Transition*

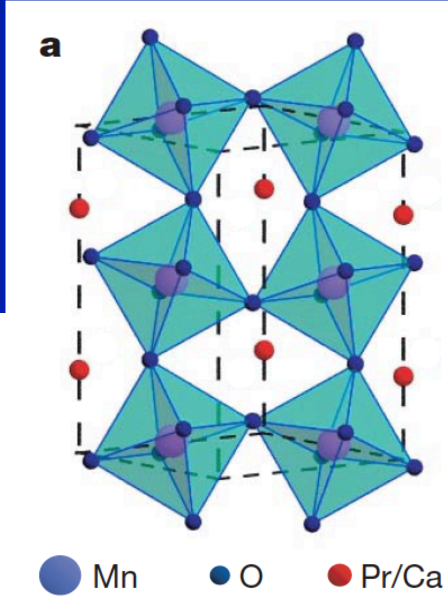

Figure 1 | $Pr_{0.7}Ca_{0.3}MnO_3$

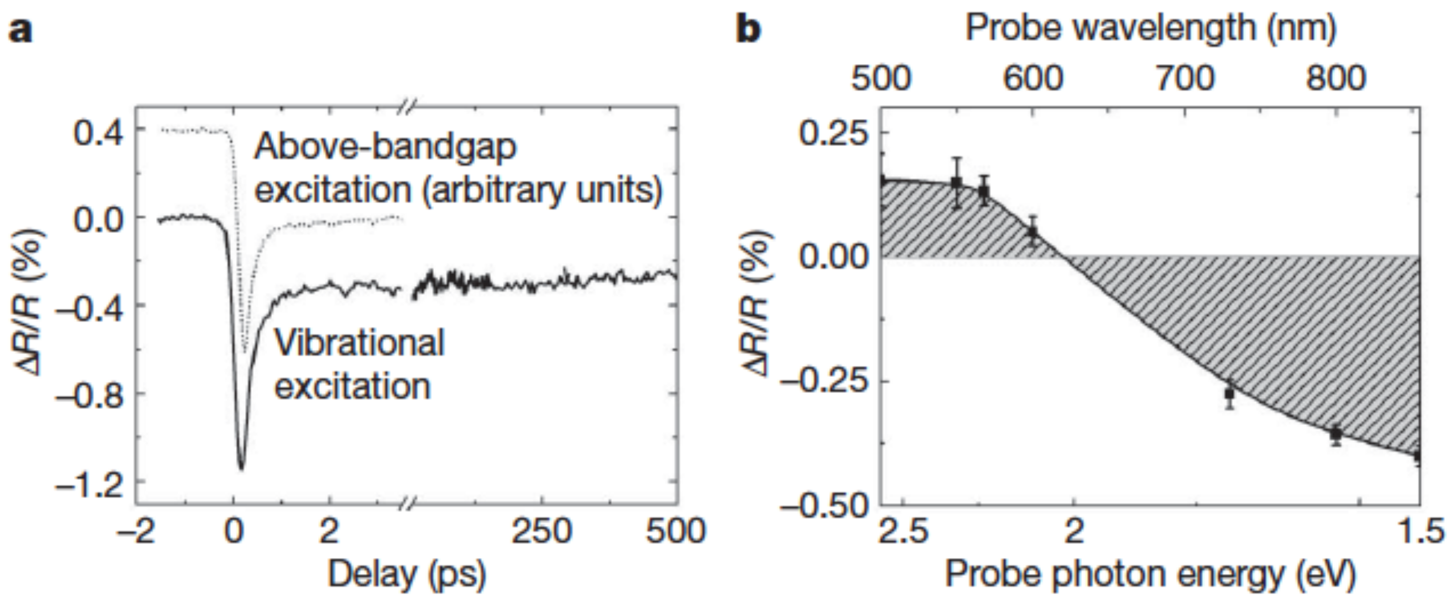

Change of reflectivity at 800nm

M. Rini et al., *Nature* 449, 72 (2007)

From other experiments (B-field): signature of metallization

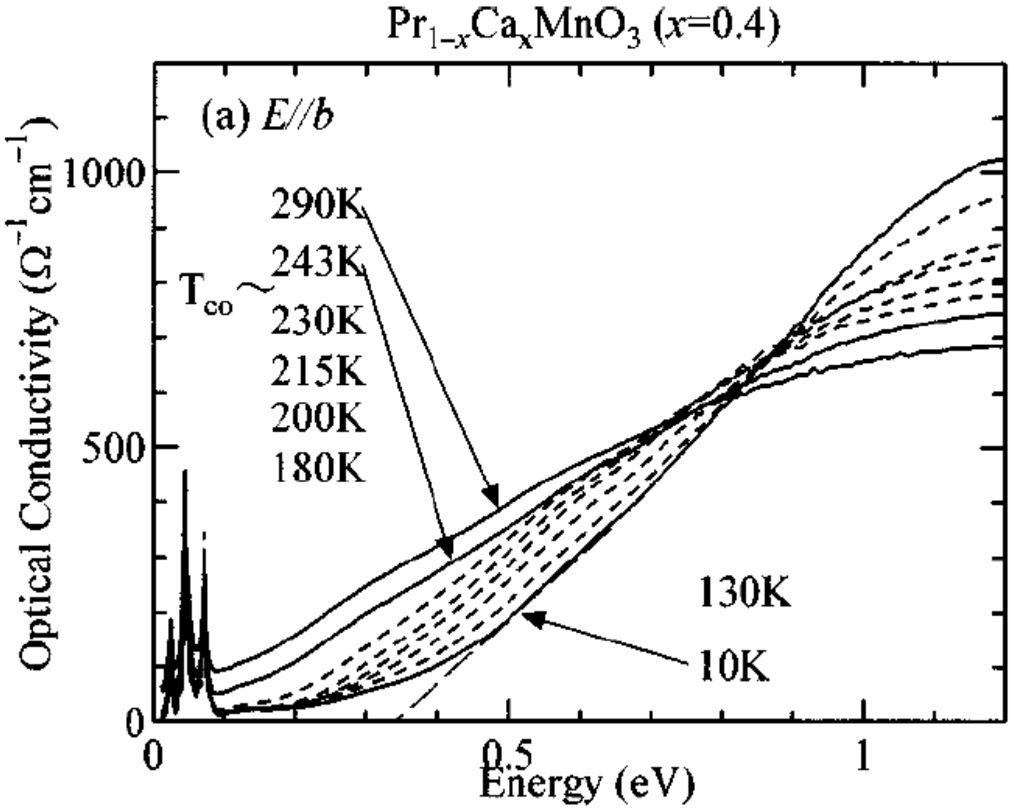

Metallization also seen Directly from Time-resolved dc-conductivity Measurement !

Note:
Optical conductivity increases above 0.8 eV as the insulating state is formed and the gap develops.

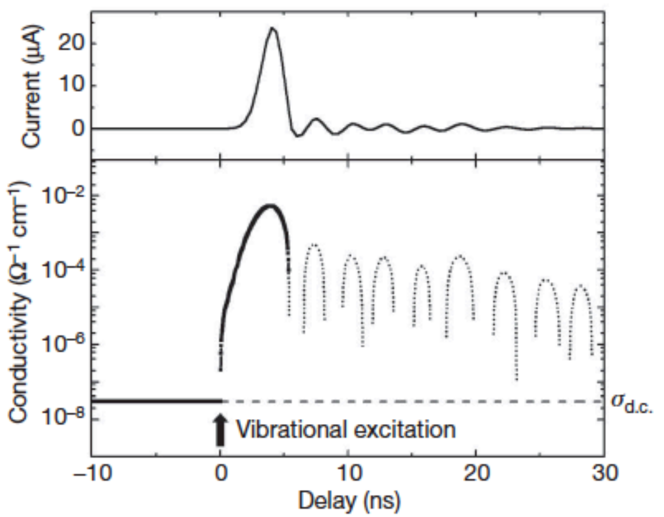

Figure 3 | Time-dependent transport measurement. Vibrational excitation of the Mn–O stretching mode results in a ~10^3 increase in the sample current (upper panel) and a corresponding ~10^5 increase in the sample conductivity (lower panel). The metastable metallic phase is formed and relaxes within the experimental time resolution of 4 ns. The current oscillations following the main pulse are due to electronic ringing and cannot be converted accurately into sample conductivity, so the derived conductivity oscillations are shown as a dotted line. The dashed line shows the d.c. conductivity of the insulating phase of $Pr_{0.7}Ca_{0.3}MnO_3$ at 30 K.

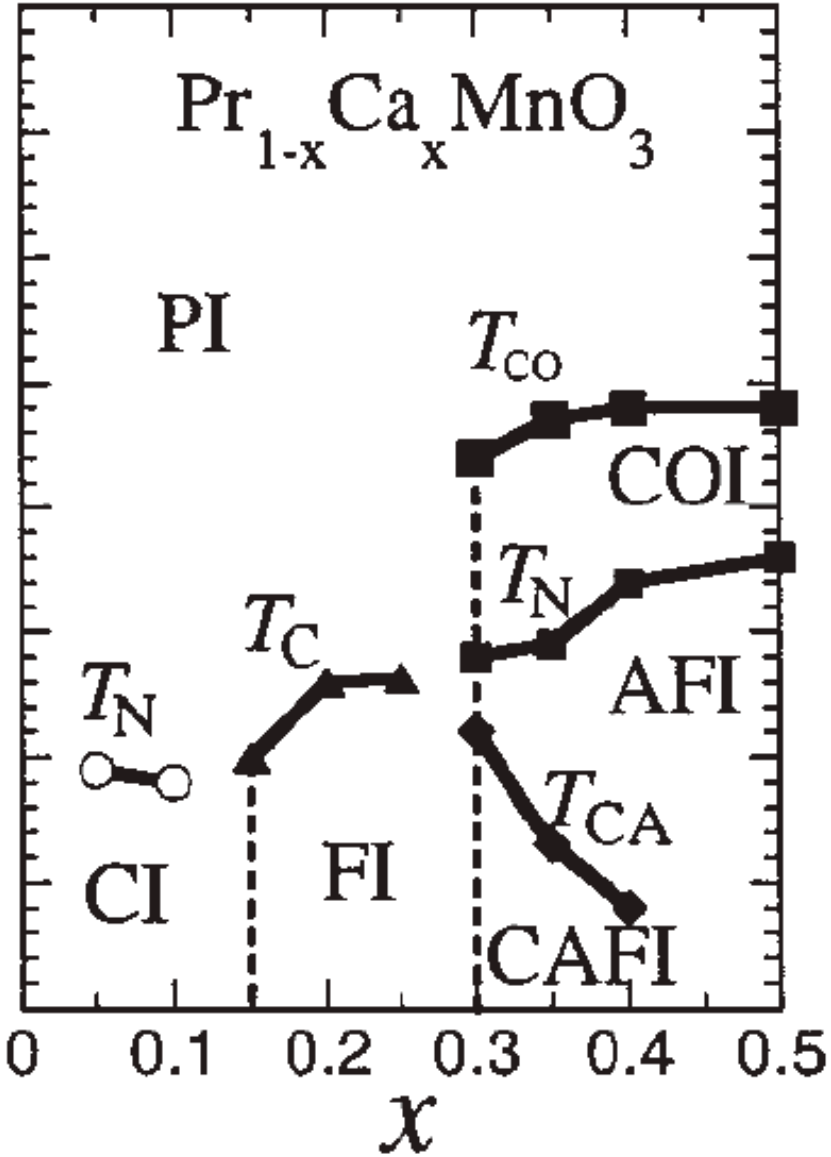

Not heating !
PCMO is an insulator for all values of x

Resonant phenomena (with ~70 meV mode)

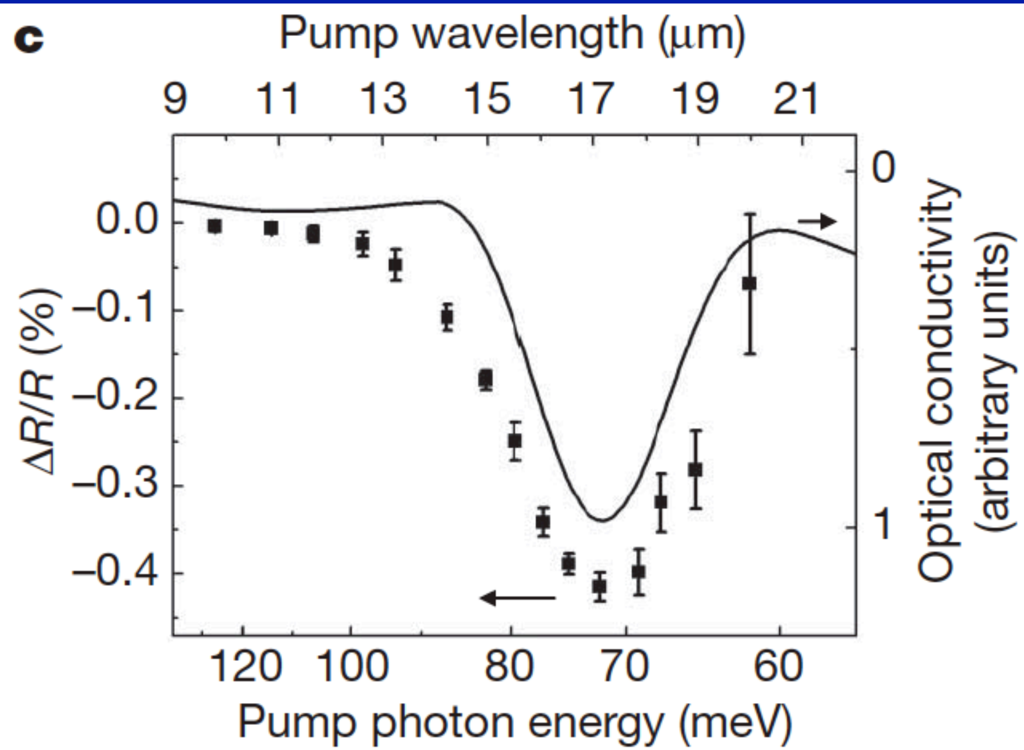

However…
Hidden metallic phase nearby

Hwang et al. PRB 52, 15046 (1995)

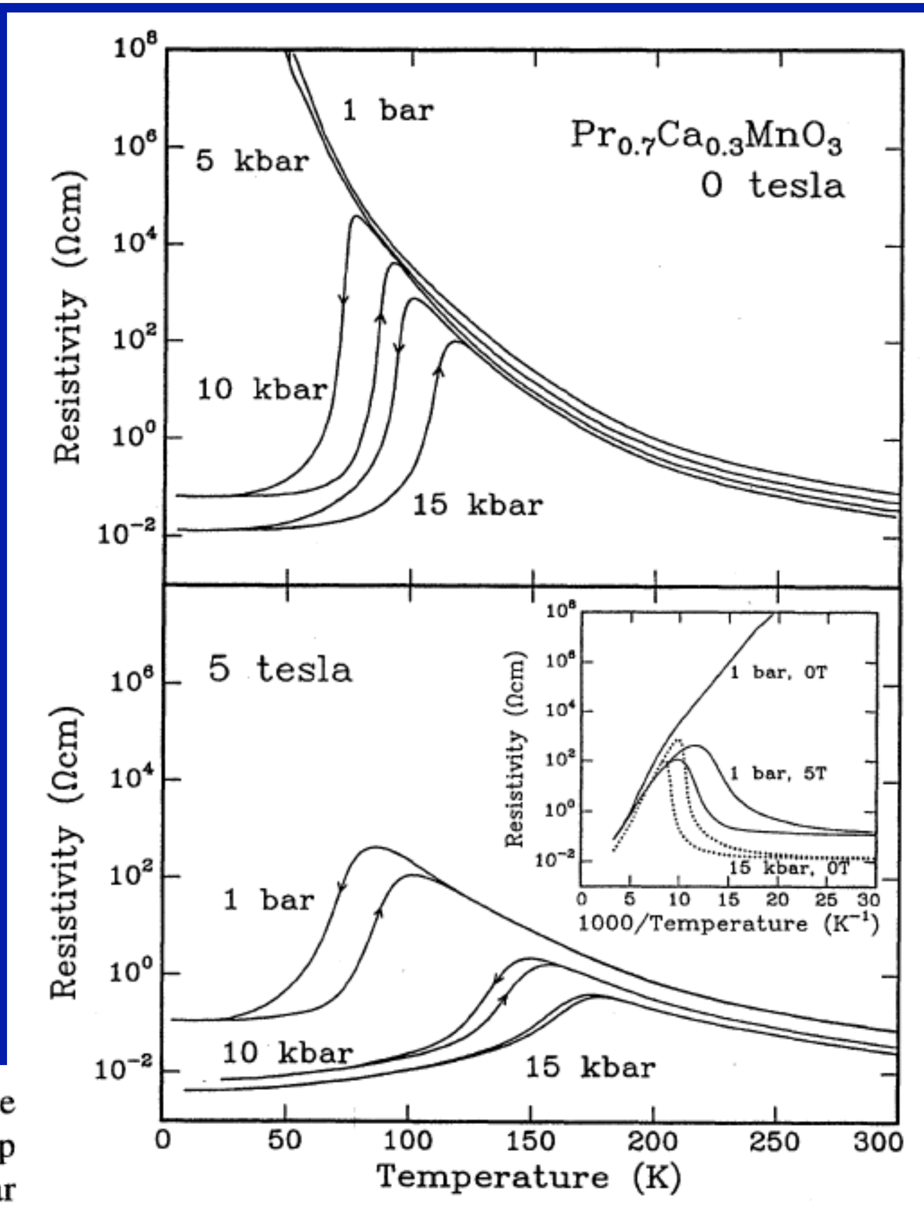

FIG. 1. The large pressure and magnetic-field sensitivity of the temperature-dependent resistivity for $Pr_{0.7}Ca_{0.3}MnO_3$. In the top panel, the resistivity is displayed on a logarithmic scale for 1 bar and 5, 10, and 15 kbar applied pressure in earth magnetic field. In the bottom panel, the resistivity is displayed on a logarithmic scale for 1 bar, 10, and 15 kbar applied pressure in 5 T field. The inset compares the effects of applying pressure and magnetic field separately by examining the resistivity on a logarithmic scale versus $1000/T$.

PUZZLE:

- Light couples directly only to dipolar-active modes

- Distortion is controlled by rotations, tilts or JT modes

- Those modes do not carry a dipolar moment !

Phonon (Raman and IR) spectroscopy

electromagnetic wave as a probe radiation (***photon – opt. phonon interaction***):

Infrared absorption: $\hbar\omega_{photon} = E_{ES}^{(phonon)} - E_{GS}^{(phonon)}$

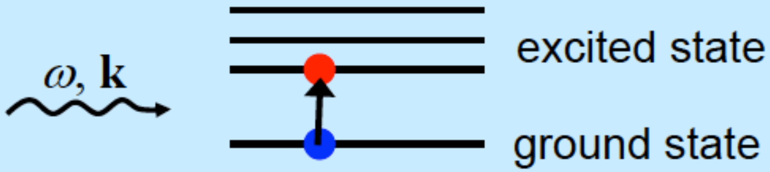

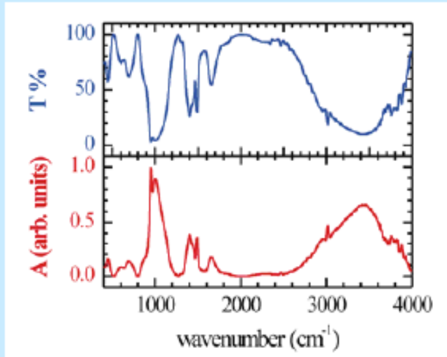

Raman scattering ≡ inelastic light scattering from optical phonons

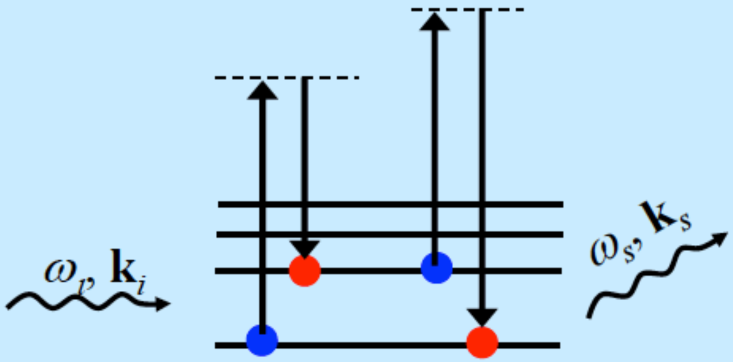

Stokes	anti-Stokes
$\omega_s = \omega_i - \Omega$	$\omega_s = \omega_i + \Omega$
$\mathbf{k}_s = \mathbf{k}_i - \mathbf{K}$	$\mathbf{k}_s = \mathbf{k}_i + \mathbf{K}$

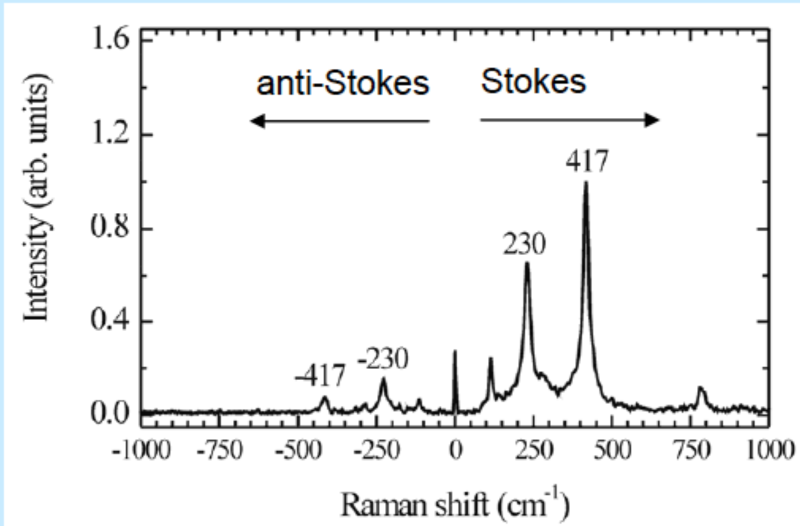

From B.Mihailova
http://www.cryst.ehu.es/html/lekeitio-docs/mihailova-presentation.pdf

Raman and IR intensities

IR activity: induced dipole moment due to the change in the atomic positions

$$\boldsymbol{\mu} = (\mu_x, \mu_y, \mu_z)$$

$$\boldsymbol{\mu}(Q) = \boldsymbol{\mu}_0 + \sum \frac{\partial \boldsymbol{\mu}}{\partial Q_k} Q_k + \ldots$$

Q_k – configurational coordinate

$\neq 0$, IR activity

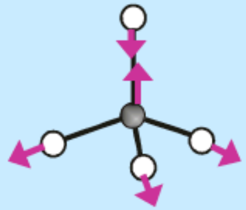

IR: “asymmetrical”, “one-directional”

Raman activity: induced dipole moment due to deformation of the e^- shell

Polarizability tensor: $\boldsymbol{\alpha} = \begin{pmatrix} \alpha_{xx} & \alpha_{xy} & \alpha_{xz} \\ \alpha_{xy} & \alpha_{yy} & \alpha_{yz} \\ \alpha_{xz} & \alpha_{yz} & \alpha_{zz} \end{pmatrix}$

$$\mathbf{P} = \boldsymbol{\alpha}.\mathbf{E}$$

induced polarization
(dipole moment per unit cell)

$$\boldsymbol{\alpha}(Q) = \boldsymbol{\alpha}_0 + \sum \frac{\partial \boldsymbol{\alpha}}{\partial Q_k} Q_k + \ldots$$

$\neq 0$, Raman activity

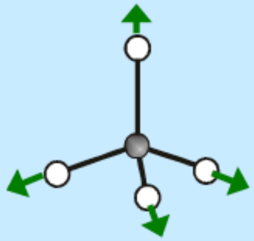

Raman: “symmetrical”, “two-directional”

N.B.! simultaneous IR and Raman activity – only in non-centrosymmetric structures

From B.Mihailova
http://www.cryst.ehu.es/html/lekeitio-docs/mihailova-presentation.pdf

“Non-Linear Phononics”

Key qualitative idea: Först et al. Nature Phys 7, 854 (2011)
Microsopic theory: Subedi, Cavalleri and AG, PRB 89 22031R (2014)

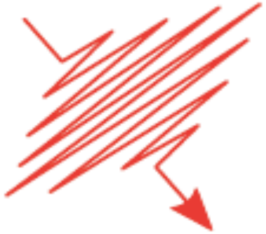

cf `Ionic Raman Scattering’

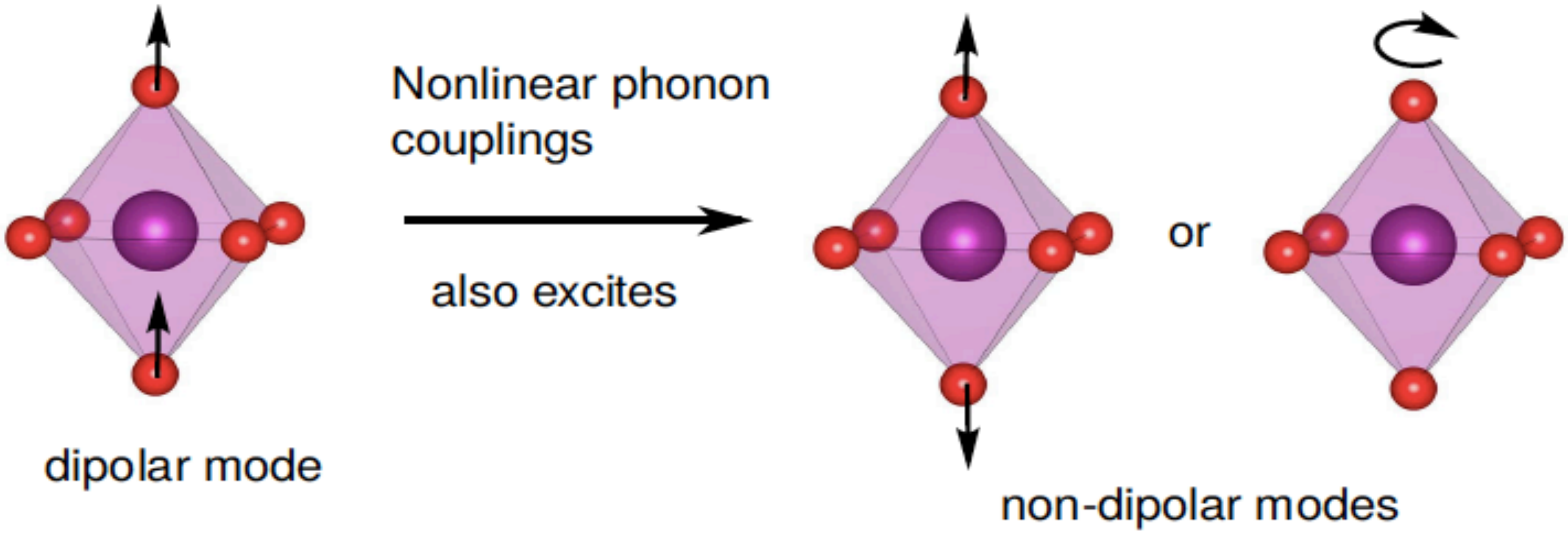

PHYSICAL REVIEW B **89**, 220301(R) (2014)

Theory of nonlinear phononics for coherent light control of solids

Alaska Subedi,[1] Andrea Cavalleri,[2,3] and Antoine Georges[1,4,5]

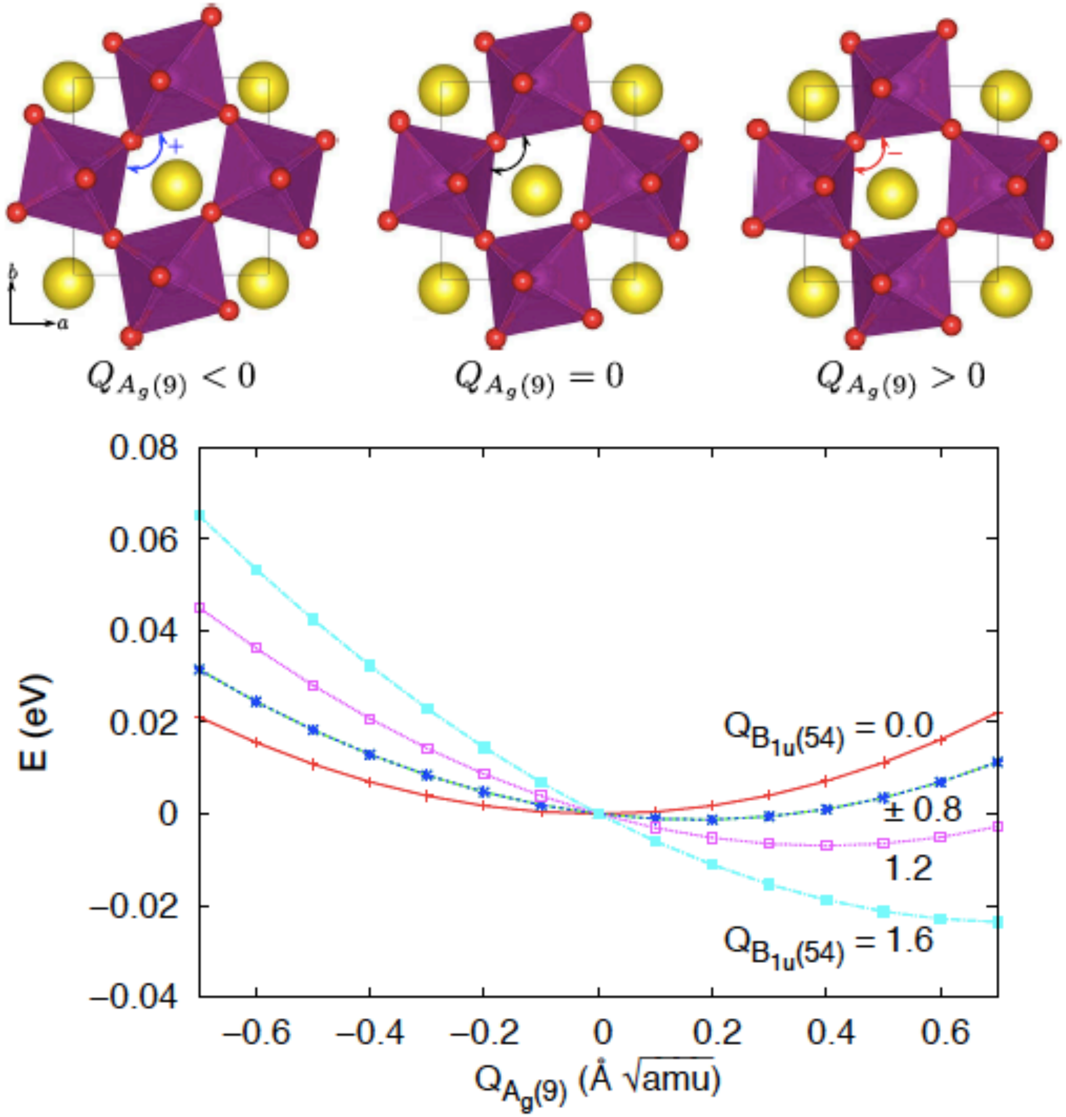

Energy surface for $PrMnO_3$ as a function of Raman mode for different amplitudes of pumped IR mode

TABLE I: Calculated zone center phonon frequencies and the symmetries of selected modes of orthorhombic $PrMnO_3$. The mode number is given in the parenthesis.

Calc. freq. (cm^{-1})		Symmetry
97.43		$A_g(4)$
154.80	Octahedral rotations ~ 19 meV	$A_g(9)$
231.10		$A_g(21)$
267.58		$A_g(23)$
351.07		$A_g(36)$
479.49		$A_g(47)$
552.09		$A_g(51)$
622.12	c-axis `shaking' of octahedra ~ 77 meV	$B_{1u}(54)$
633.38		$B_{1u}(56)$
639.95		$B_{2u}(58)$
660.54		$B_{3u}(60)$

NL coupling to a symmetry-preserving Raman mode: cubic

$$V(Q_{\mathrm{R}}, Q_{\mathrm{IR}}) = \frac{1}{2}\Omega_{\mathrm{R}}^2 Q_{\mathrm{R}}^2 + \frac{1}{2}\Omega_{\mathrm{IR}}^2 Q_{\mathrm{IR}}^2 + \frac{1}{3}a_3 Q_{\mathrm{R}}^3 + \frac{1}{4}b_4 Q_{\mathrm{IR}}^4$$
$$\boxed{-\frac{1}{2}g\, Q_{\mathrm{R}} Q_{\mathrm{IR}}^2} \qquad (1)$$

Transforms as a scalar under point group – see below

$$\ddot{Q}_{\mathrm{IR}} + \Omega_{\mathrm{IR}}^2 Q_{\mathrm{IR}} = g\, Q_{\mathrm{R}} Q_{\mathrm{IR}} - b_4 Q_{\mathrm{IR}}^3 + F(t)$$
$$\ddot{Q}_{\mathrm{R}} + \Omega_{\mathrm{R}}^2 Q_{\mathrm{R}} = \frac{1}{2}g\, Q_{\mathrm{IR}}^2 - a_3 Q_{\mathrm{R}}^2 .$$

Note: $Q_{IR}^2(t) \propto \cos^2 \Omega_{IR} t$ has a finite mean-value !

Effective potential seen by Raman mode, time-averaged over IR mode:

$$V_{\text{eff}}(Q_{\text{R}}) = \frac{1}{2}\Omega_{\text{R}}^2 Q_{\text{R}}^2 + \frac{1}{3}a_3 Q_{\text{R}}^3 - \frac{1}{4} g Q_{\text{IR,max}}^2 Q_{\text{R}} \quad (11)$$

The displaced position δQ_{R} corresponds to the minimum of this potential given by $a_3 \delta Q_{\text{R}}^2 + \Omega_{\text{R}}^2 \delta Q_{\text{R}} - g Q_{\text{IR,max}}^2/4 = 0$, and thus reads

$$\begin{aligned} \delta Q_{\text{R}} &= \frac{\Omega_{\text{R}}^2}{2a_3}\left[\sqrt{1 + \frac{a_3 g Q_{\text{IR,max}}^2}{\Omega_{\text{R}}^4}} - 1\right] \quad (12) \\ &\simeq \frac{g}{4\Omega_{\text{R}}^2} Q_{\text{IR,max}}^2 - \frac{1}{16} a_3 \frac{g^2 Q_{\text{IR,max}}^4}{\Omega_{\text{R}}^6} + \cdots \end{aligned}$$

The mechanism:

Upon pumping (fast IR mode),
the effective potential seen by the slow (Raman-active) mode has a shifted minimum, corresponding to a change of the structure

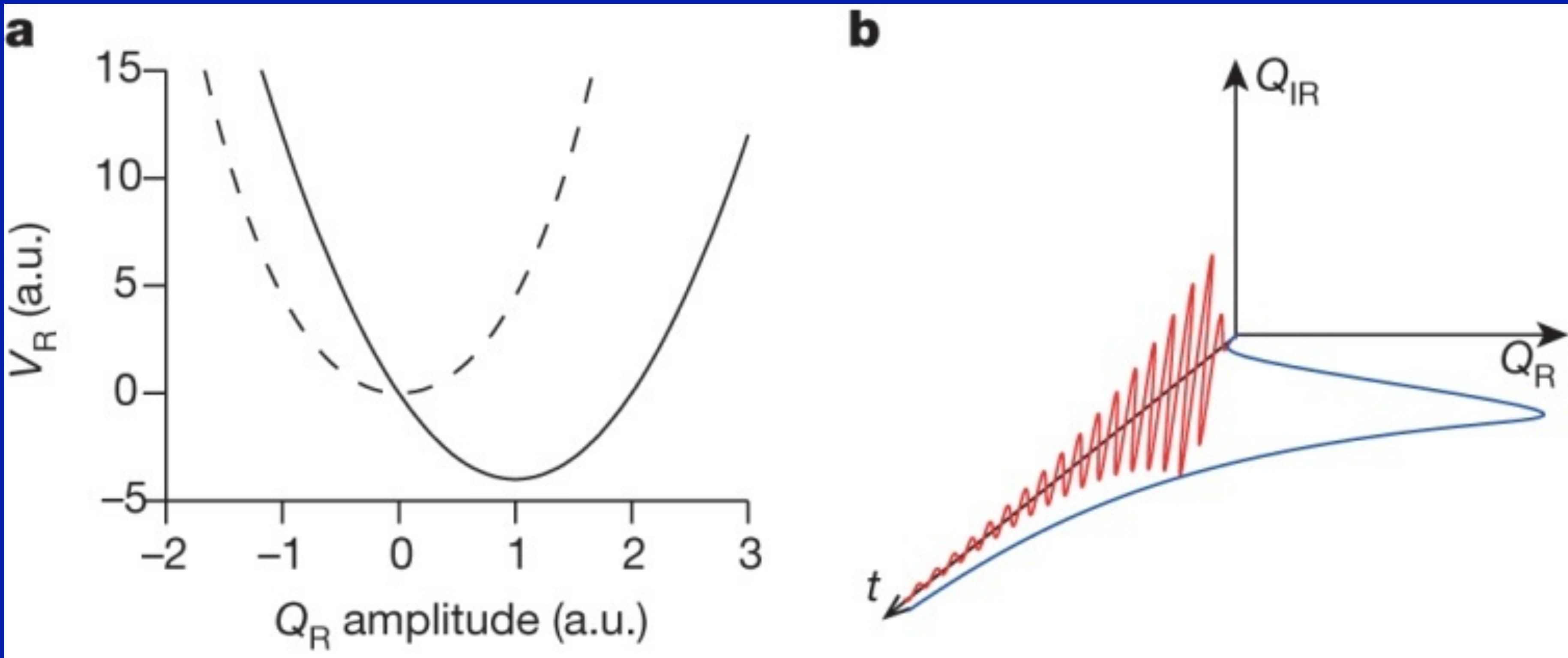

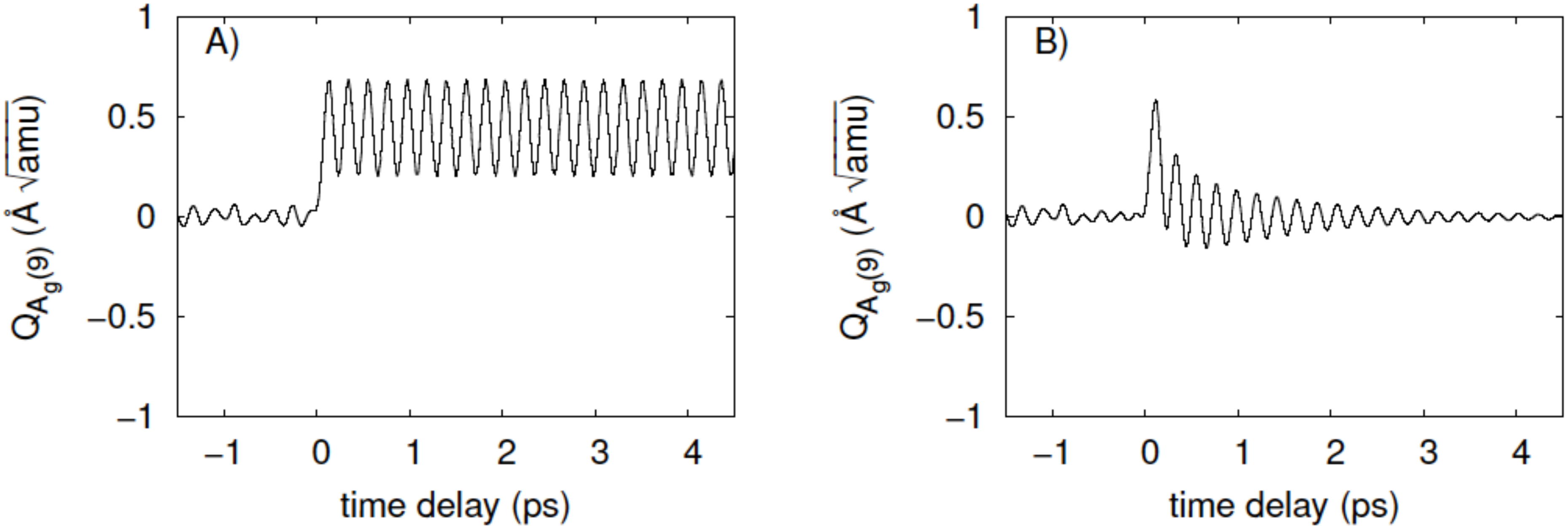

FIG. 5: Dynamics of the Raman $A_g(9)$ mode for PMO (cubic coupling). Left panel: dynamics without damping. Right panel: dynamics with damping values of 5% for both $B_{1u}(54)$ and $A_g(9)$ modes.

Displacement of the Raman phonon away from equilibrium position

$$\begin{aligned} \ddot{Q}_{\rm IR} + \Omega_{\rm IR}^2 Q_{\rm IR} &= g\, Q_{\rm R} Q_{\rm IR} - b_4 Q_{\rm IR}^3 + F(t) \\ \ddot{Q}_{\rm R} + \Omega_{\rm R}^2 Q_{\rm R} &= \frac{1}{2} g\, Q_{\rm IR}^2 - a_3 Q_{\rm R}^2 \,. \end{aligned}$$

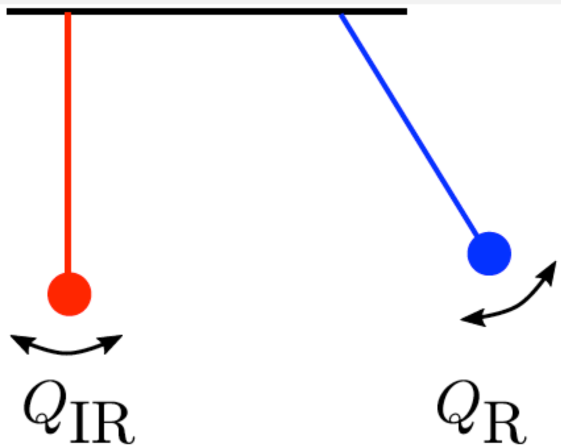

Reducing orthorombic distortion increases bandwidth and leads to metallic phase
(can be quantified by a DMFT+DFT calculation:)

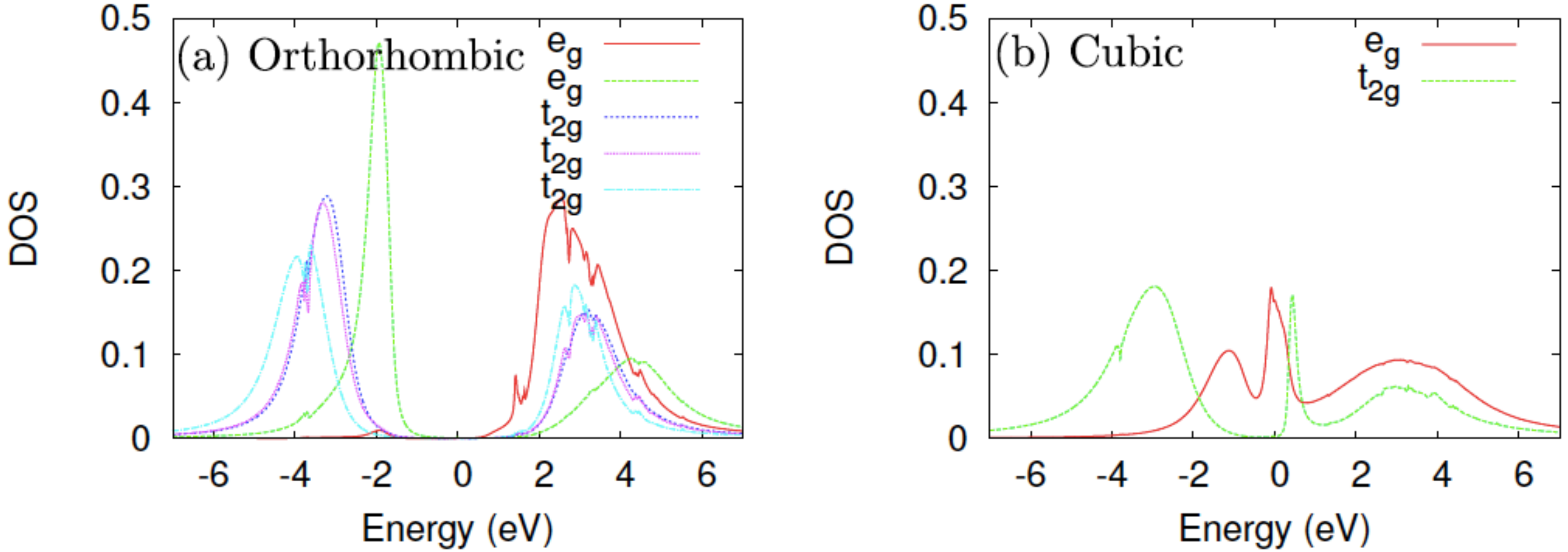

- May explain experimental observation of Rini et al.
- However: is the 'undistortion' large enough, given fluence ?
- Provides a quantitative framework to predict <u>how the structure changes upon resonant excitation of the IR mode</u>

Reminder: The two effects of distortion.

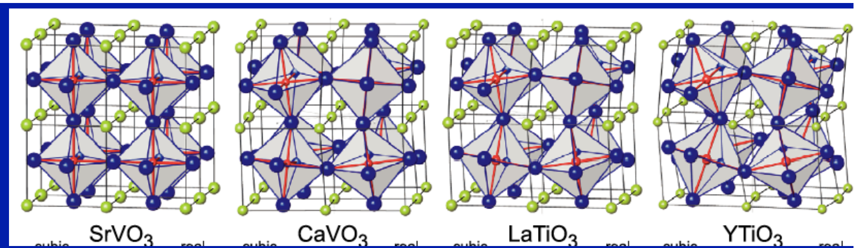

- 1) Reduction of total t_{2g} bandwidth:

Table 8. t_{2g} edge-to-edge ($W_{t_{2g}}$) and rms (W) bandwidths in eV.

	$SrVO_3$ [42]	$CaVO_3$ [43]	$LaTiO_3$ [44]	$LaTiO_3$ [12]	$YTiO_3$ [20]
$W_{t_{2g}}$	2.85	2.45	2.09	1.92	2.05
W	2.85	2.39	2.18	2.08	1.87

This is because the O-M-O bond is no longer straight
→ pi-bonding less efficient

2) Splitting between t_{2g} orbitals (<u>lifting of orbital degeneracy</u>)

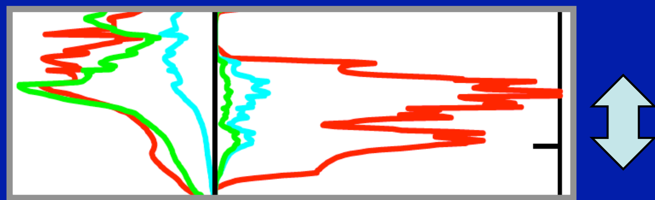

(140,200) meV for LaTiO3 ;
(200,330) meV for YTiO3

→***Both effects*** are responsible for the Mott insulating nature of $LaTiO_3$ and $YTiO_3$ (see below)

Coupling to a symmetry-breaking Raman mode:

Q^2Q^2 coupling

→ a different universality class !

Non-perturbative phenomena

…yet to be demonstrated experimentally.

However, raises issues with possible excitations of pairs of phonons (k,-k)…

La_2CuO_4

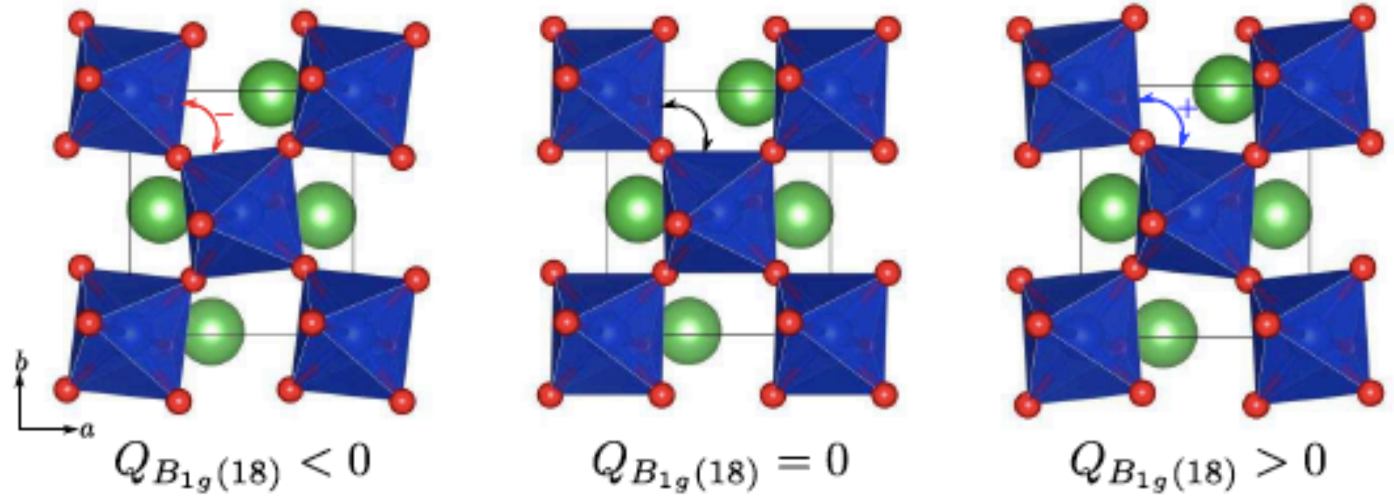

FIG. 2: Top: Sketch of the atomic displacements corresponding to the $B_{1g}(18)$ Raman mode in La_2CuO_4, illustrating the symmetry between a negative and positive displacement. Bottom: Total energy as a function of the $B_{1g}(18)$ amplitude for several values of the $B_{3u}(41)$ amplitude. For visual clarity, we plot $V(Q_R, Q_{IR}) - V(0, Q_{IR})$ so that all curves coincide at $Q_R = 0$.

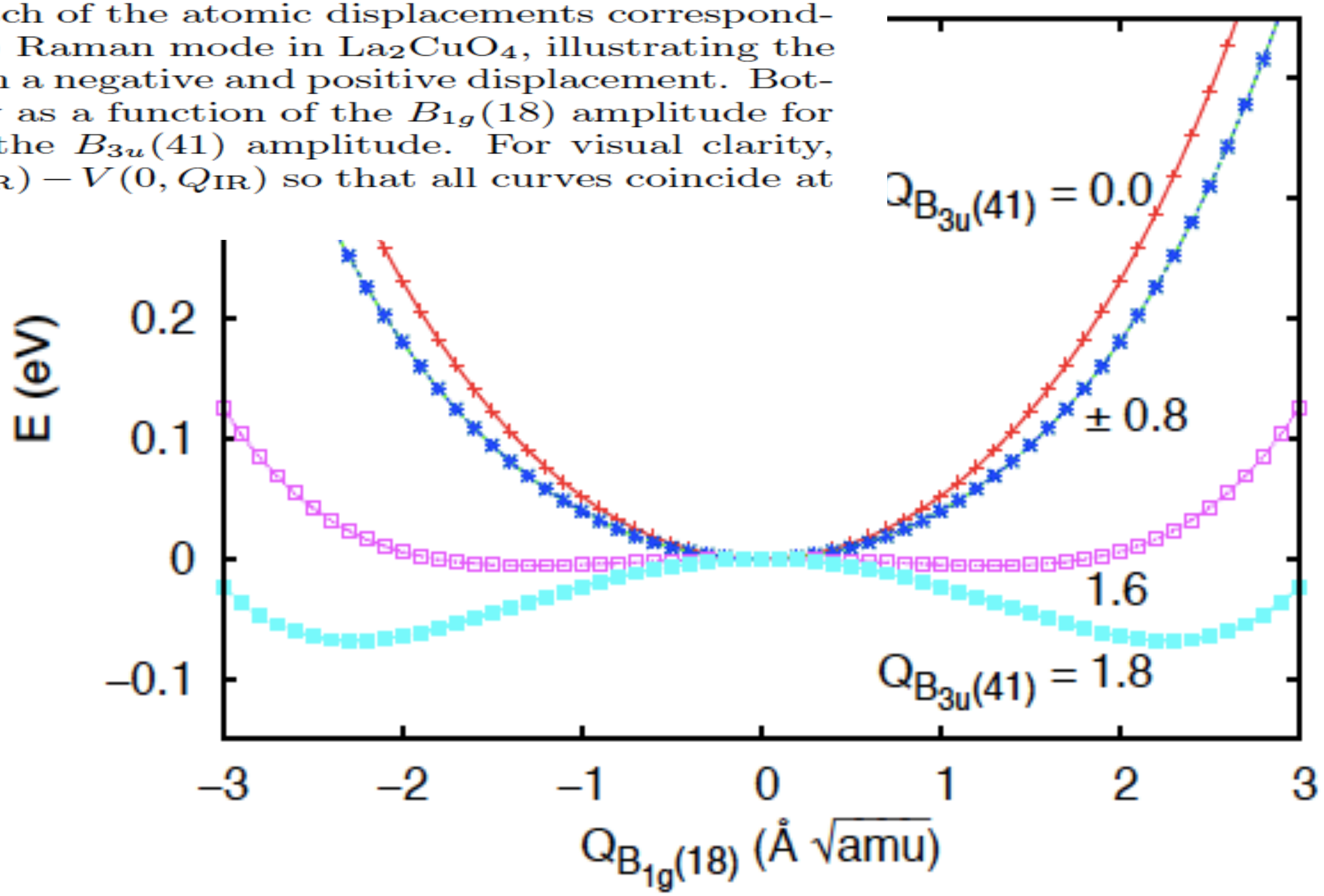

Symmetry analysis

- A_g: Identity representation. +Q and –Q not related by symmetry → Different energies → Odd powers allowed
- B_{1u} or B_{1g}: Breaks the symmetry. Structures with +Q and –Q are related by symmetry. Hence have equal energies and only even powers are allowed

$$A_g \subset A_g \otimes B_{1u} \otimes B_{1u} \quad (PrMnO_3)$$

$$A_g \subset B_{1g} \otimes B_{1g} \otimes B_{3u} \otimes B_{3u} \quad (La_2CuO_4)$$

Q^2Q^2 coupling, parametric oscillators, Kapitza pendulum and all that…

$$V(Q_\mathrm{R}, Q_\mathrm{IR}) = \frac{1}{2}\Omega_\mathrm{R}^2 Q_\mathrm{R}^2 + \frac{1}{2}\Omega_\mathrm{IR}^2 Q_\mathrm{IR}^2 + \frac{1}{4}a_4 Q_\mathrm{R}^4 + \frac{1}{4}b_4 Q_\mathrm{IR}^4 - \frac{1}{2}g\, Q_\mathrm{R}^2 Q_\mathrm{IR}^2 . \qquad (2)$$

$$\ddot{Q}_\mathrm{IR} + \Omega_\mathrm{IR}^2 Q_\mathrm{IR} = g\, Q_\mathrm{R}^2 Q_\mathrm{IR} - b_4 Q_\mathrm{IR}^3 + F(t)$$

$$\ddot{Q}_\mathrm{R} + \Omega_\mathrm{R}^2 Q_\mathrm{R} = g\, Q_\mathrm{R} Q_\mathrm{IR}^2 - a_4 Q_\mathrm{R}^3$$

Very different type of coupling: ~ parametric oscillator
Frequency softening. Dynamical instability. Mathieu equation

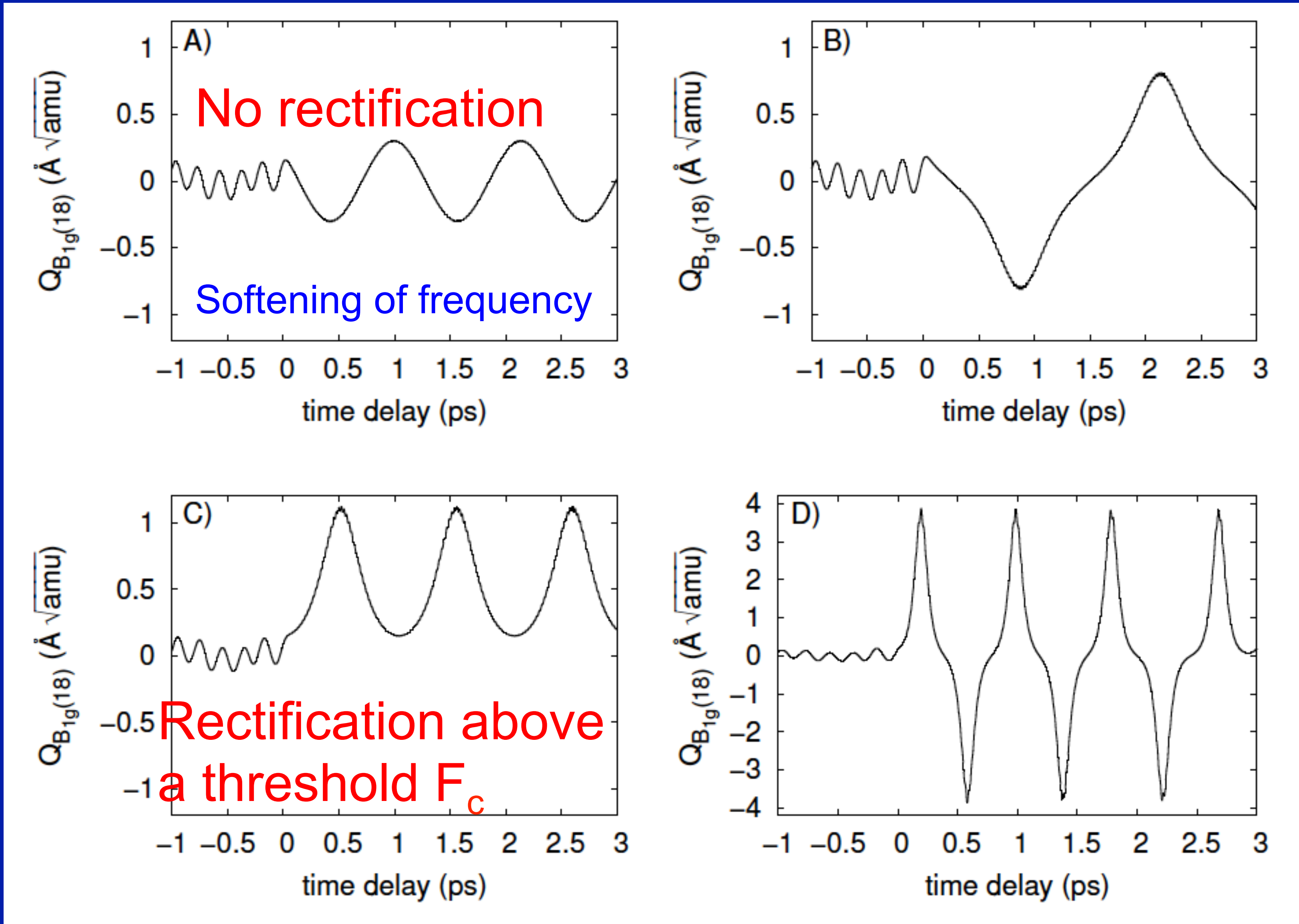

Softening of the Raman mode, Dynamical threshold for displacement (driven parametric oscillator)

$$V_{\text{eff}}(Q_{\text{R}}) = \frac{1}{2}\Omega_{\text{R}}^2 Q_{\text{R}}^2 \left[1 - \frac{gQ_{\text{IR,max}}^2}{2\Omega_{\text{R}}^2}\right] + \frac{1}{4}a_4 Q_{\text{R}}^4 \qquad (16)$$

Softening of frequency

The motion becomes unstable when this effective potential acquires a negative curvature, so that to first approximation (ie neglecting corrections of order $\Omega_{\text{R}}/\Omega_{\text{IR}} \ll 1$, see below) the instability threshold is given by:

$$\Omega_{R,\text{eff}} = \Omega_{\text{R}} \left[1 - \frac{gQ_{\text{IR,max}}^2}{2\Omega_{\text{R}}^2}\right]^{1/2} = \Omega_{\text{R}} \sqrt{1 - \frac{F^2}{F_c^2}}$$

$$\frac{gQ_{\text{IR,max}}^2}{2\Omega_{\text{R}}^2} = 1 \Rightarrow$$

$$\Rightarrow F_c = \sqrt{\frac{2}{g}} \frac{\Omega_{\text{R}}}{\Omega_{\text{IR}}} \left[\int_{-\infty}^{+\infty} d\tau \tau^2 \Phi(\tau)\right]^{-1} = \frac{\Omega_{\text{R}}}{\Omega_{\text{IR}}} \frac{1}{\sqrt{\pi g \sigma^3}}$$

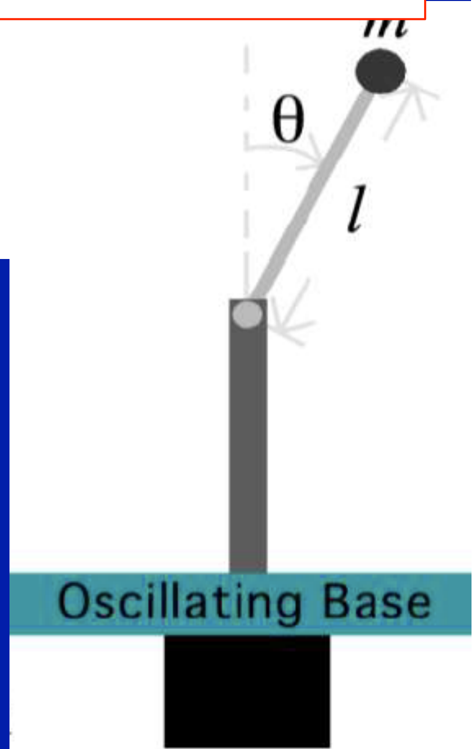

Dynamical stabilization: the dynamical threshold is larger than that corresponding to the instability of the static potential $(F_c/\sqrt{2} \ \ vs. \ \ F_c)$
cf. Kapitza's pendulum

Driven systems: new energy landscapes

Take a pendulum and vibrate its pivot point:

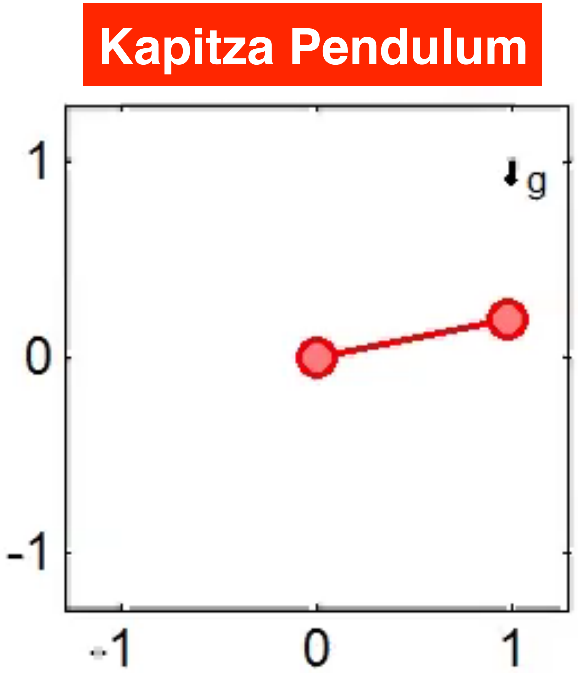

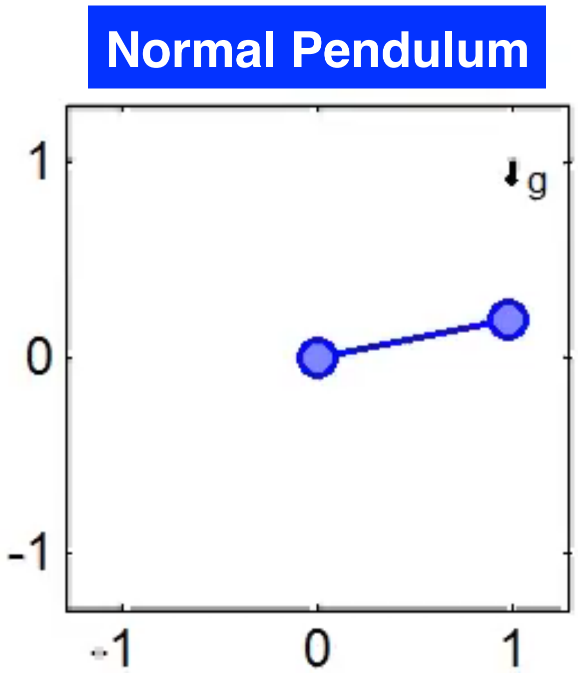

P.L. Kapitza, "Dynamic stability of a pendulum with an oscillating point of suspension," ***Zh. Eksp. Teor. Fiz.*** **21, 588 (1951)**

L.D. Landau and E.M. Lifschitz ***Mechanics*** **(Pergamon, Oxford 1976)**

Slide: courtesy A.Cavalleri

Direct experimental probe of
Non-Linear Phononics
(Mechanism and Theory)

Time-resolved X-ray diffraction
(@ Free-Electron Lasers)

→ Direct evidence of displacement of
Raman modes

Free Electron Lasers

X-ray Lasers

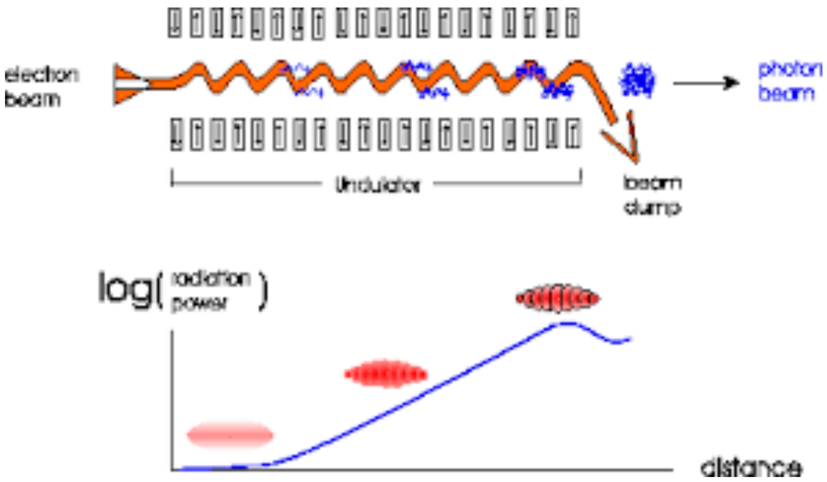

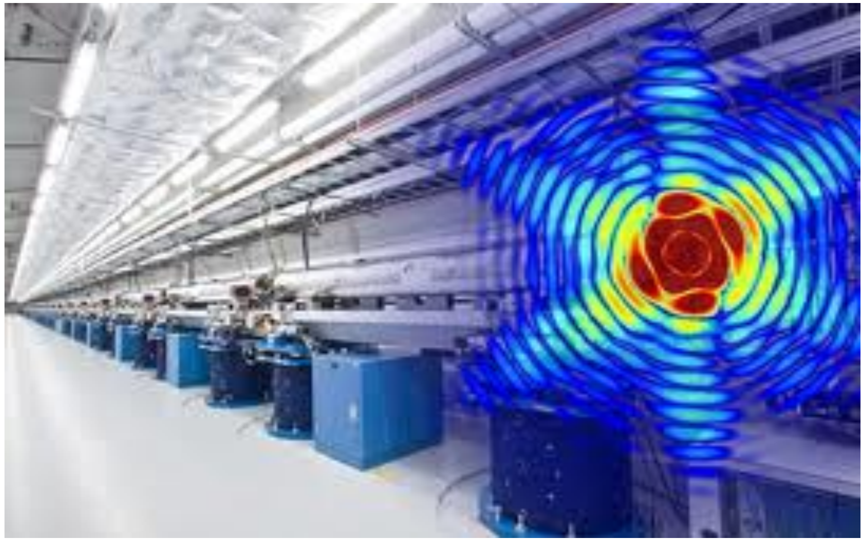

Allow for studying how the structure evolves in time

Slide from A.Cavalleri's lectures

Step change in structure factor: $La_{0.7}Sr_{0.3}MnO_3$

Mid-IR pump (E_{1u} mode)

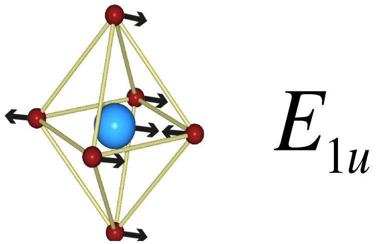

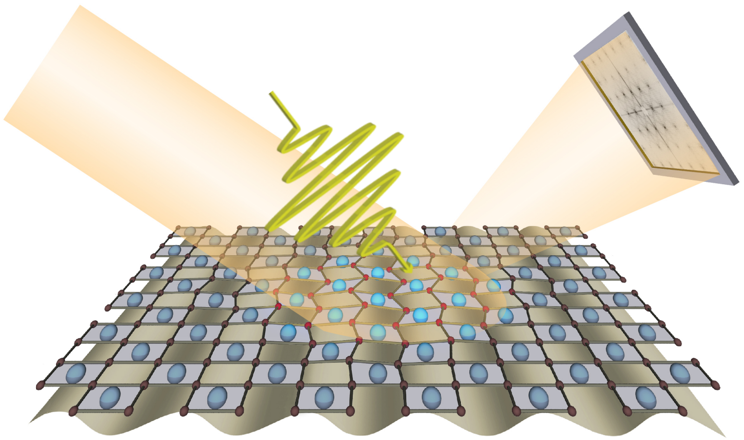

Displacive field (E_g mode)

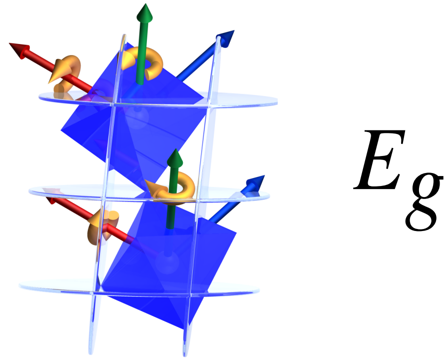

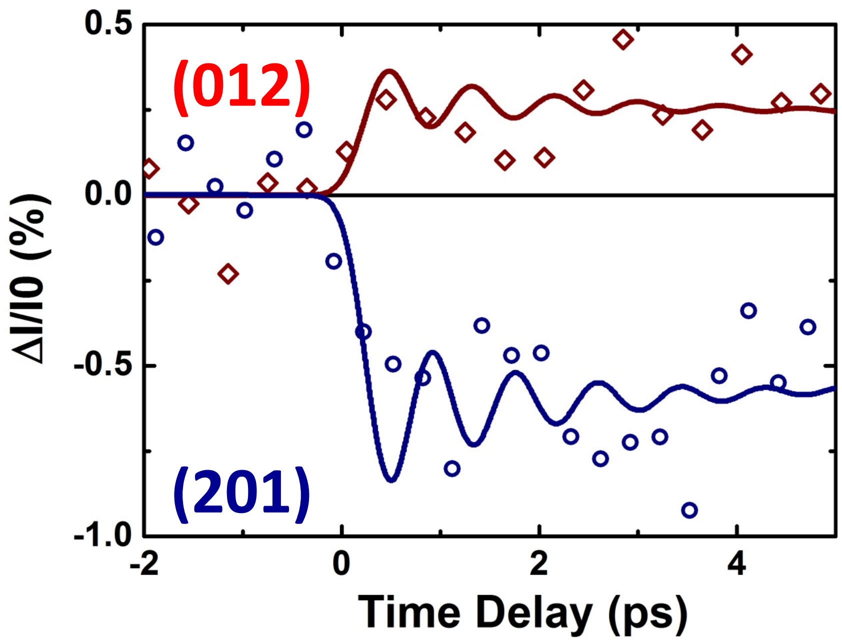

M. Foerst et al. Solid State Comm. 169, 4 (2013)

Revealing the light-induced structural changes: Non-Linear Phononics of YBCO

(time-resolved X-ray and theory)

LETTER

Roman Mankowsky
Alaska Subedi

doi:10.1038/nature13875

Nonlinear lattice dynamics as a basis for enhanced superconductivity in $YBa_2Cu_3O_{6.5}$

R. Mankowsky[1,2,3]*, A. Subedi[4]*, M. Först[1,3], S. O. Mariager[5], M. Chollet[6], H. T. Lemke[6], J. S. Robinson[6], J. M. Glownia[6], M. P. Minitti[6], A. Frano[7], M. Fechner[8], N. A. Spaldin[8], T. Loew[7], B. Keimer[7], A. Georges[4,9,10] & A. Cavalleri[1,2,3,11]

Pump 20THz B_{1u} mode: shaking apical oxygens

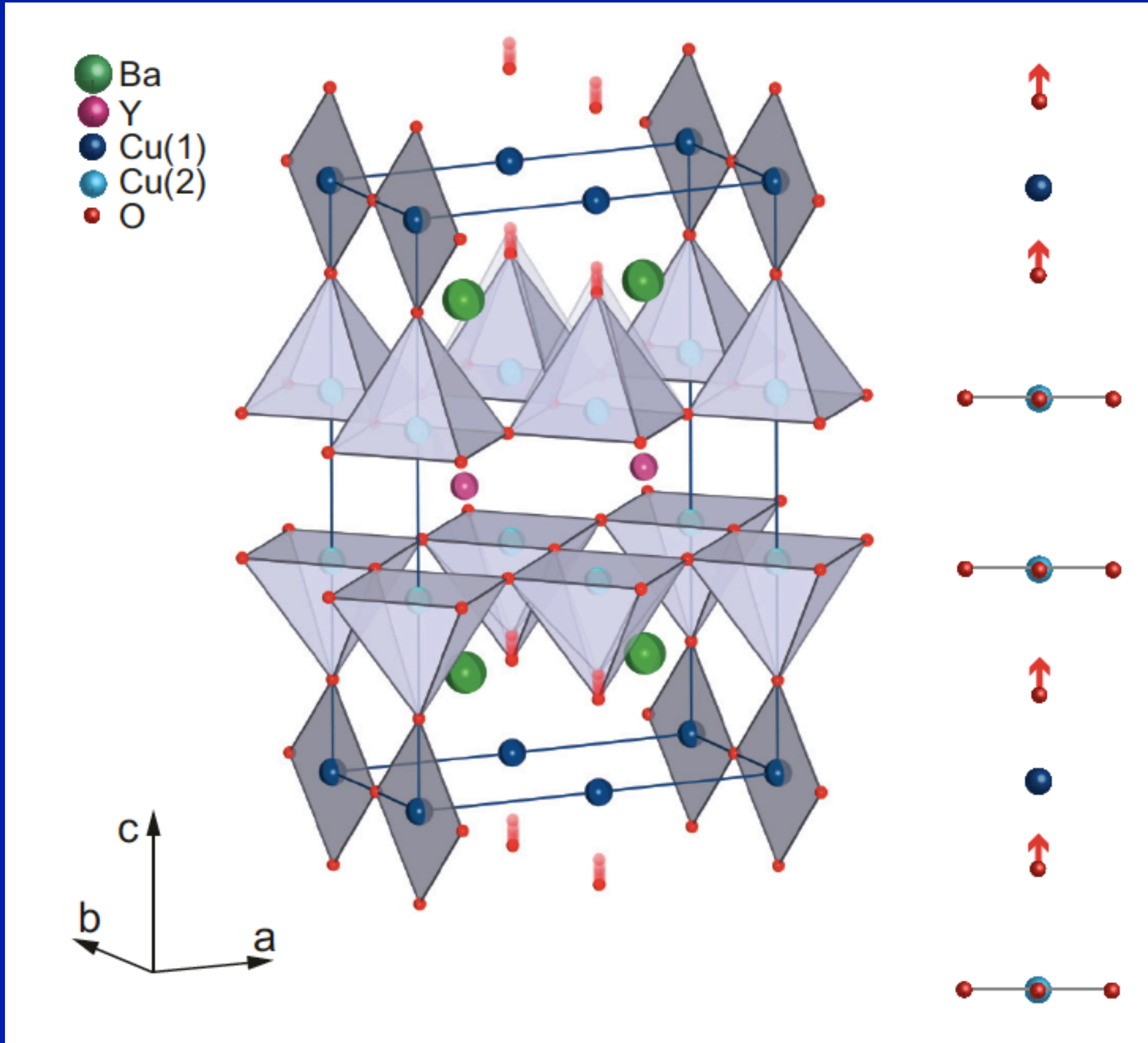

Time-resolved measurements of 4 Bragg peaks

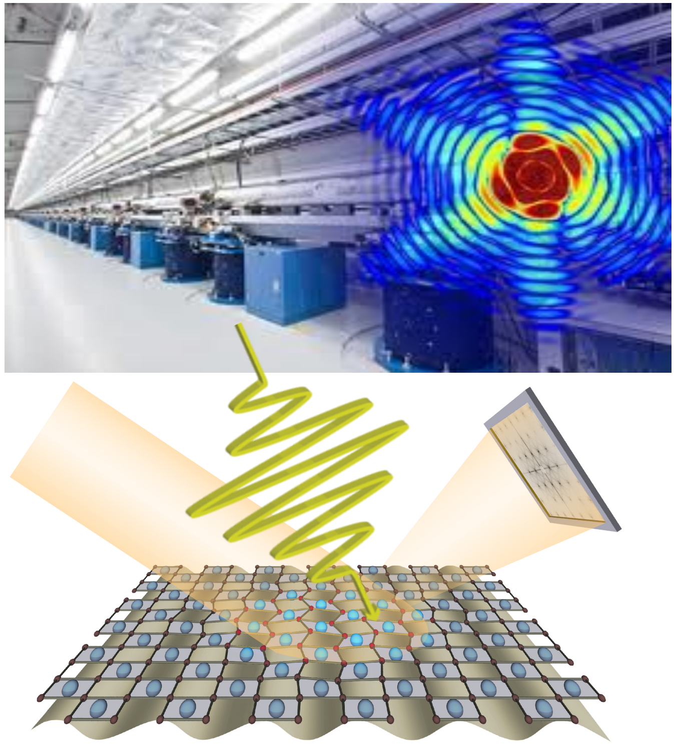

(0,-1,4)

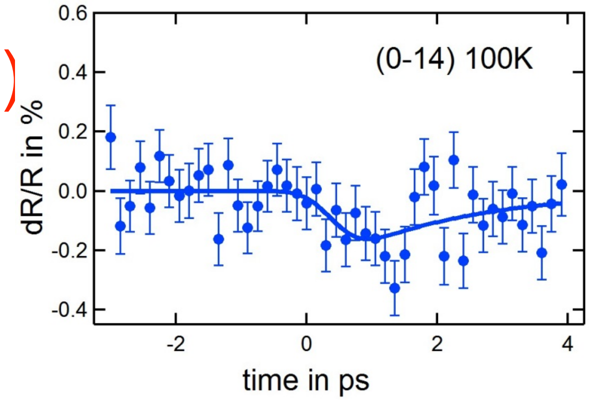

(-1,0,4)

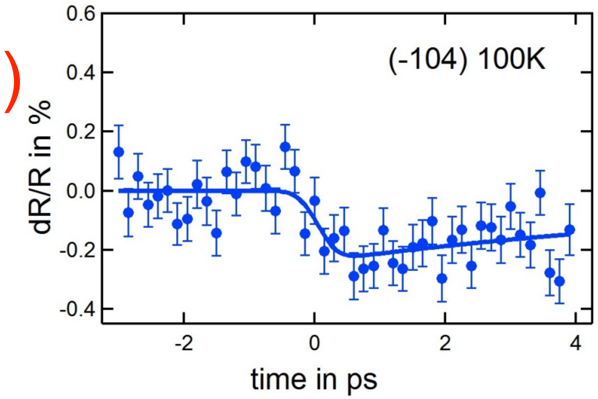

(-1,1,1)

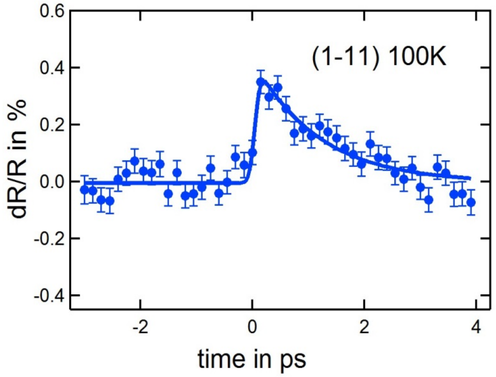

(1,-1,1)

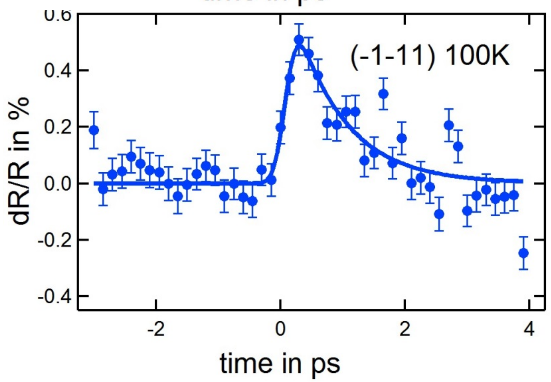

Slide courtesy A.Cavalleri ;R. Mankowski et al. *Nature* (2014)

A zoo of phonons…

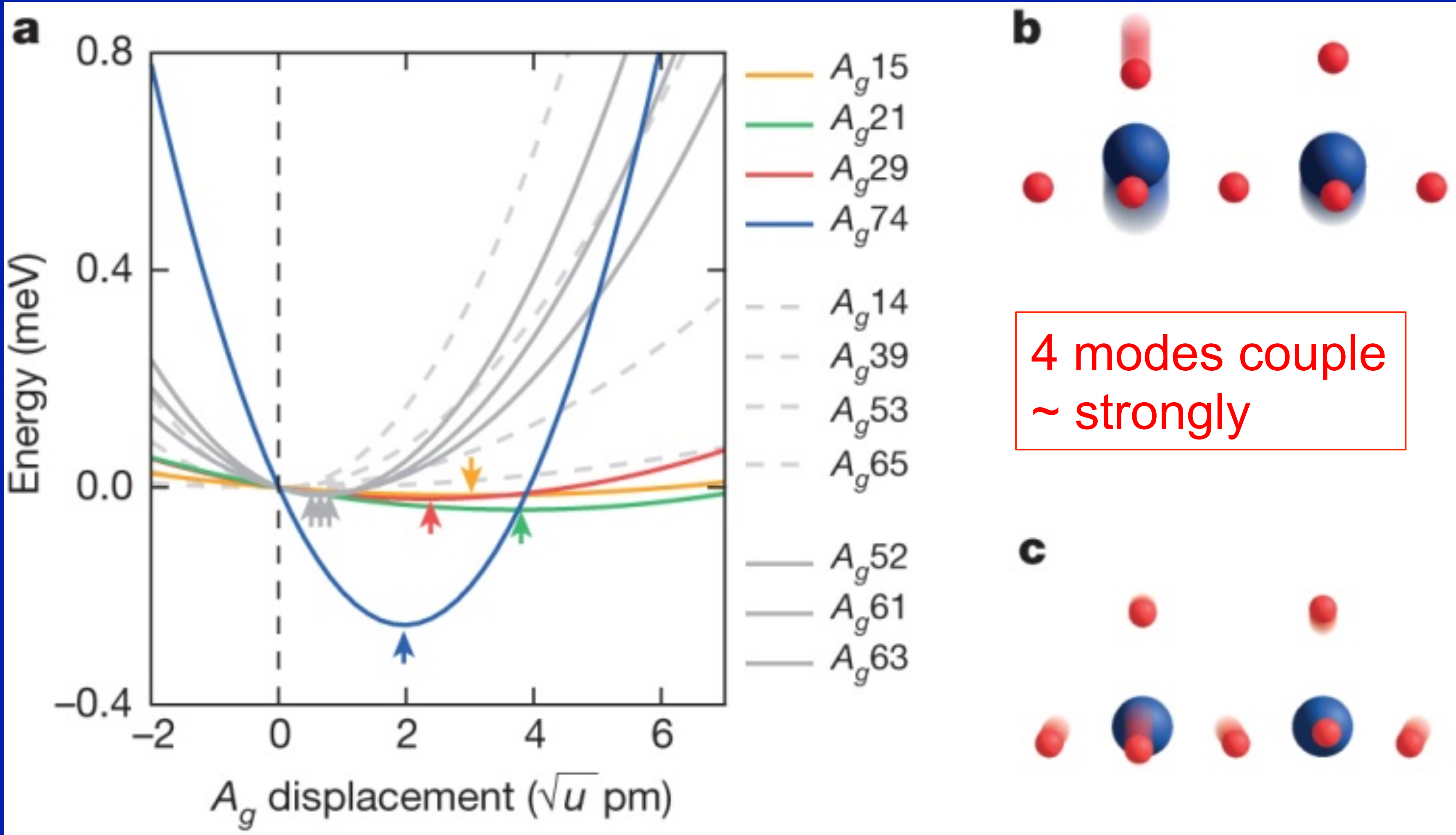

4 modes couple
~ strongly

Fit of experiment to theory:

1 overall amplitude (and 2 decay constants)

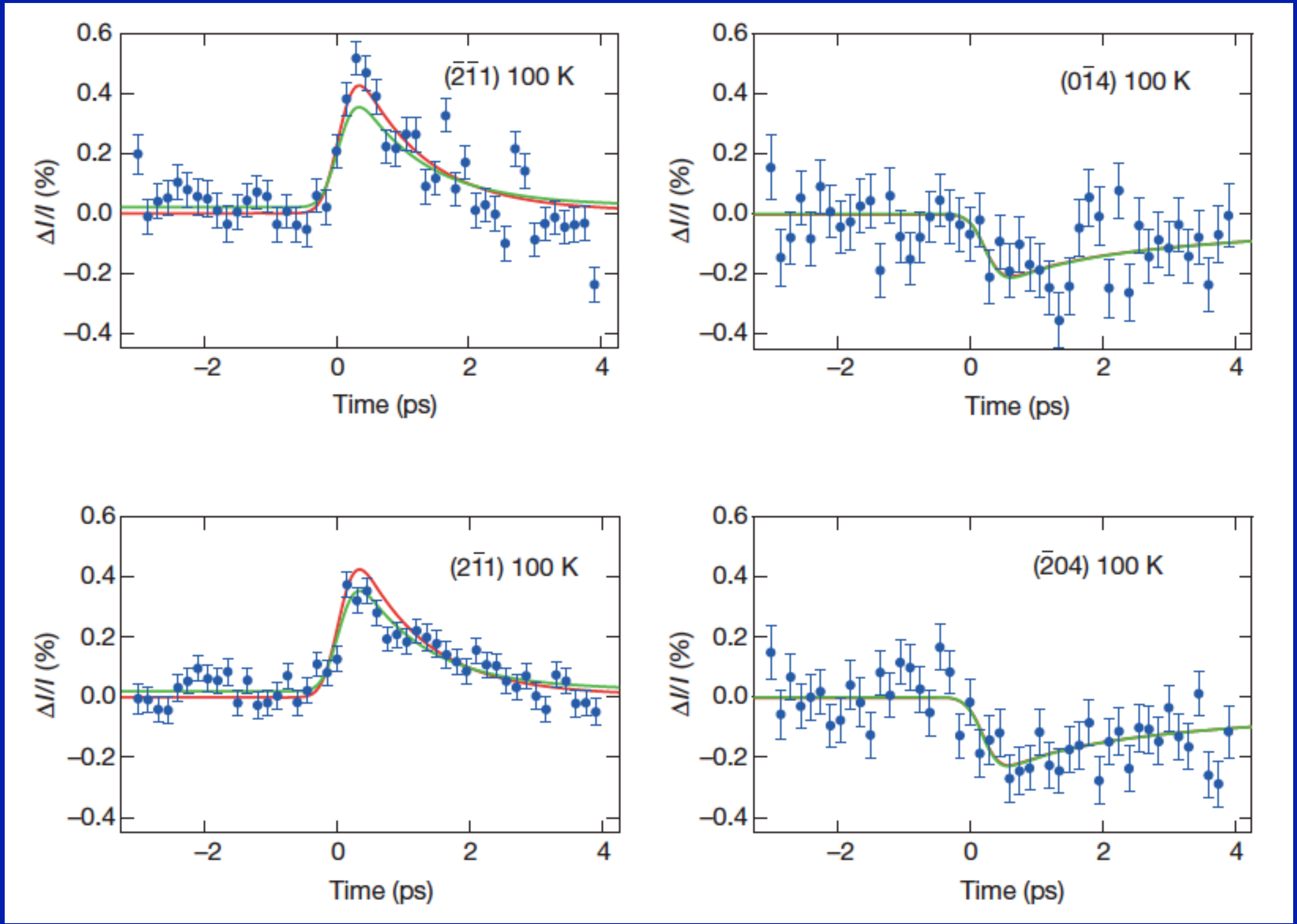

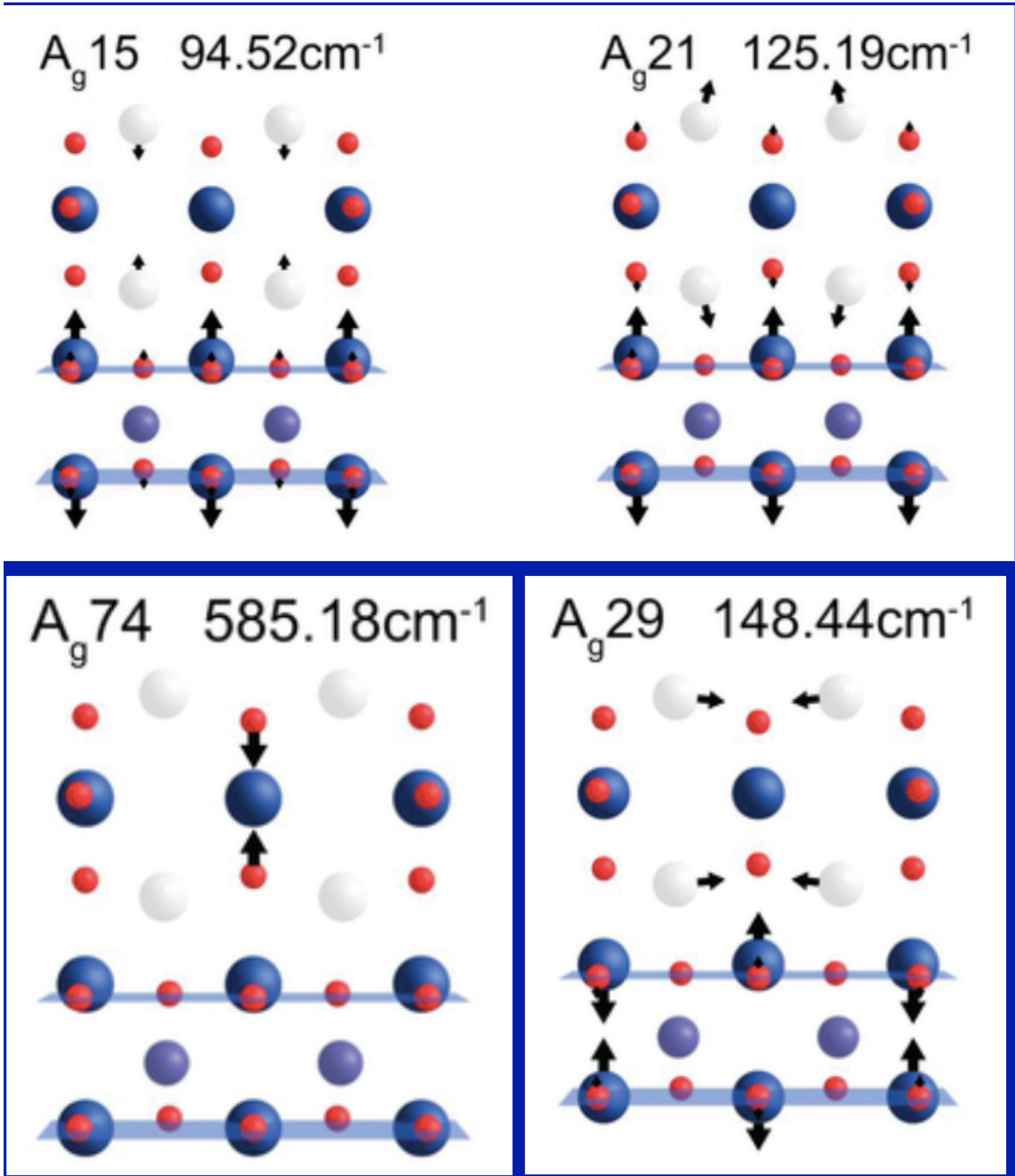

- Buckling of planes INCREASES
- Apical oxygen distance DECREASES slightly (~pm)
- Staggered motion of planes:

intra-bilayer distance increases

Inter bilayer decreases

From Light-induced MIT…
… to Light-induced Superconductivity

Light-Induced Superconductivity in a Stripe-Ordered Cuprate
D. Fausti *et al.*
Science **331**, 189 (2011);
DOI: 10.1126/science.1197294

Light-induced SC in CUPRATES

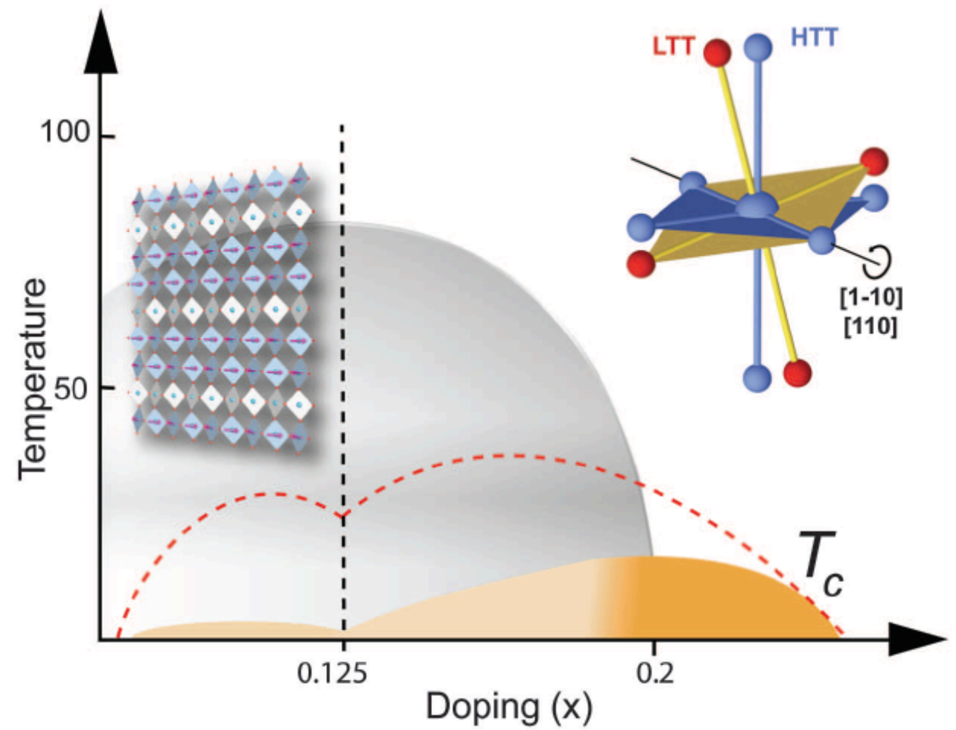

Fig. 1. Schematic phase diagram for $La_{1.8-x}Eu_{0.2}Sr_xCuO_4$. Superconductivity (yellow area) is quenched at all doping levels (gray area) below 0.2, emerging only at very low temperatures. At 0.125 doping, a static 1D modulation of charges and spins, the stripe state, emerges in the planes. This stripe phase (left inset) is associated with a LTT distortion, in which the oxygen octahedrals in the crystal are tilted (right inset). The red dashed curve marks the boundary for superconductivity in compounds of the type $La_{2-x}Sr_xCuO_4$, in which the LTT structural modulation is less pronounced.

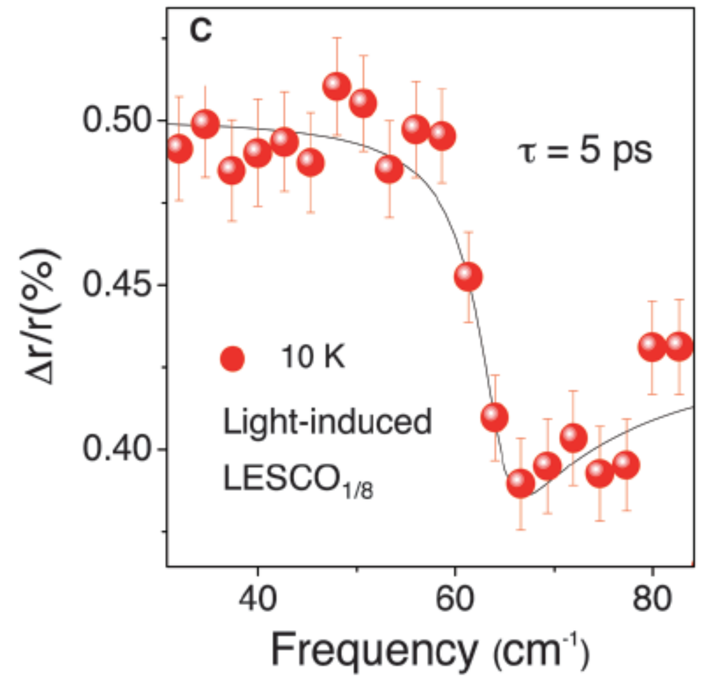

compound down to the lowest temperatures. (**C**) Transient *c*-axis reflectance of $LESCO_{1/8}$, normalized to the static reflectance. Measurements are taken at 10 K, after excitation with IR pulses at 16 μm wavelength. The appearance of a plasma edge at 60 cm^{-1} demonstrates that the photoinduced state is superconducting.

Report of Light-induced SC in YBCO far above T_c !

arXiv:1205.4661

PHYSICAL REVIEW B **89**, 184516 (2014)

Optically induced coherent transport far above T_c in underdoped $YBa_2Cu_3O_{6+\delta}$

S. Kaiser,[1,*] C. R. Hunt,[1,4] D. Nicoletti,[1] W. Hu,[1] I. Gierz,[1] H. Y. Liu,[1] M. Le Tacon,[2] T. Loew,[2] D. Haug,[2] B. Keimer,[2] and A. Cavalleri[1,3,†]

nature materials

ARTICLES

PUBLISHED ONLINE: 11 MAY 2014 | DOI: 10.1038/NMAT3963

Optically enhanced coherent transport in $YBa_2Cu_3O_{6.5}$ by ultrafast redistribution of interlayer coupling

W. Hu[1†], S. Kaiser[1†], D. Nicoletti[1†], C. R. Hunt[1,2†], I. Gierz[1], M. C. Hoffmann[1], M. Le Tacon[3], T. Loew[3], B. Keimer[3] and A. Cavalleri[1,4★]

Light-induced SC in Fullerenes

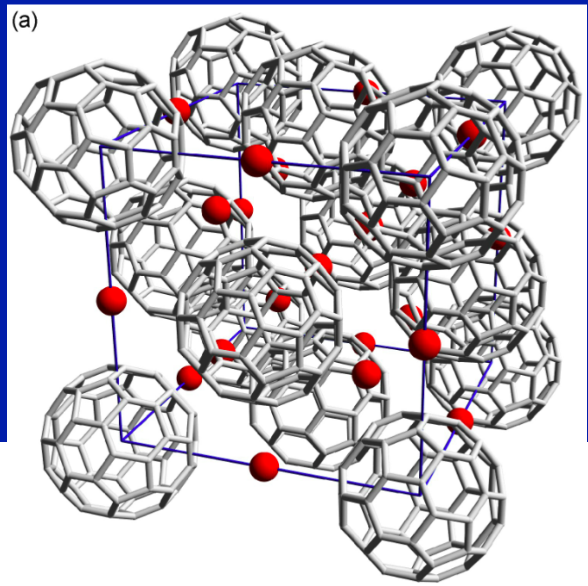

Nature 530, 461 (2016)

LETTER

doi:10.1038/nature16522

Possible light-induced superconductivity in K_3C_{60} at high temperature

M. Mitrano[1], A. Cantaluppi[1,2], D. Nicoletti[1,2], S. Kaiser[1], A. Perucchi[3], S. Lupi[4], P. Di Pietro[3], D. Pontiroli[5], M. Riccò[5], S. R. Clark[1,6,7], D. Jaksch[7,8] & A. Cavalleri[1,2,7]

Superconducting-like light-induced state

K_3C_{60}

Cooling

Photo-excitation

T = 5 x T_c

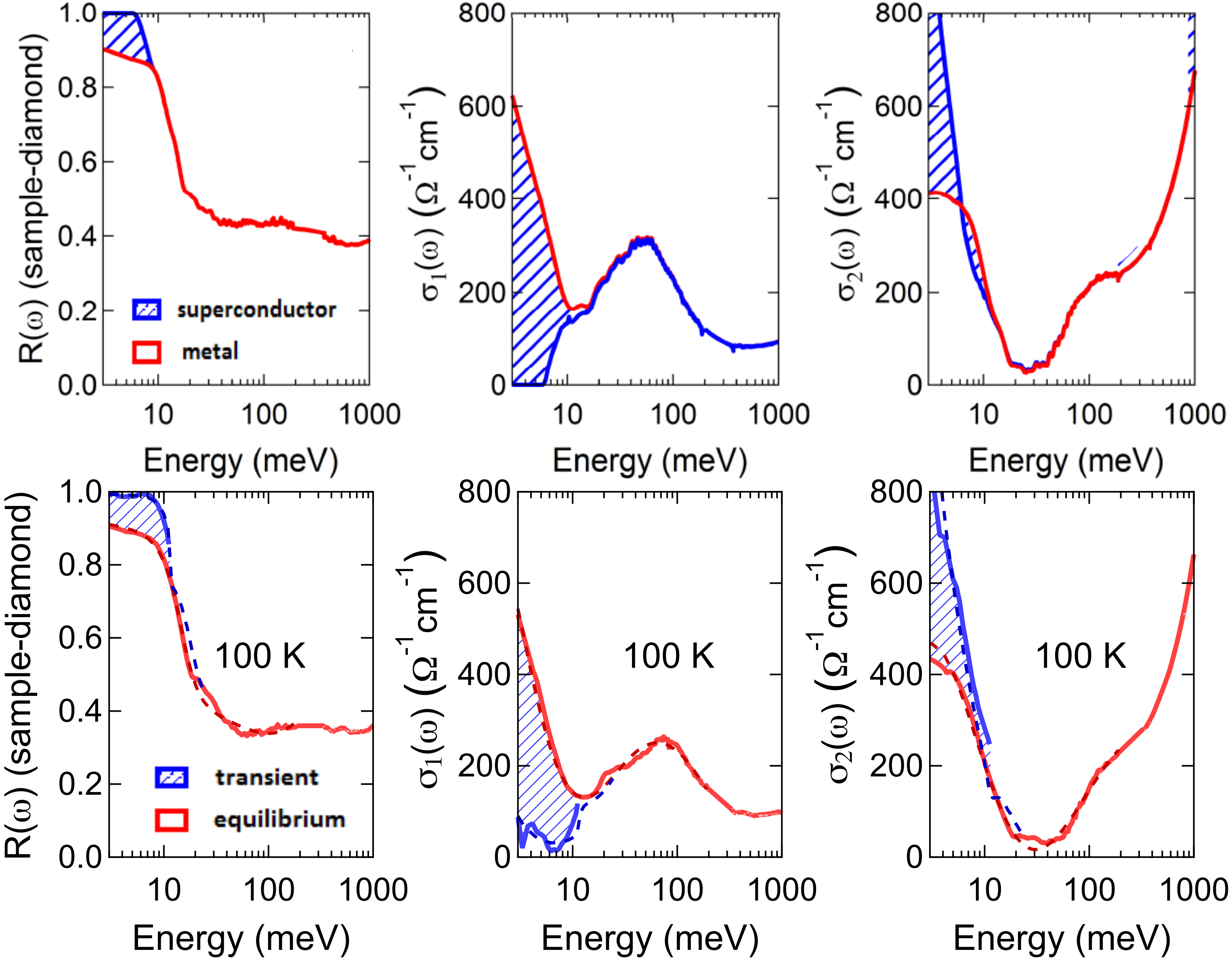

Direct driving: modulating U

PRL **115,** 187401 (2015) PHYSICAL REVIEW LETTERS week ending 30 OCTOBER 2015

THz-Frequency Modulation of the Hubbard *U* in an Organic Mott Insulator

R. Singla,[1,*] G. Cotugno,[1,2] S. Kaiser,[1,7,8,†] M. Först,[1] M. Mitrano,[1] H. Y. Liu,[1] A. Cartella,[1] C. Manzoni,[1,4] H. Okamoto,[5] T. Hasegawa,[6] S. R. Clark,[2,9] D. Jaksch,[2,3] and A. Cavalleri[1,2,‡]

$$H_{e-ph} = \sum_i \hat{n}_i \left[A_1 Q_i + A_2 Q_i^2 + \cdots\right] + \sum_i \hat{n}_{i\uparrow}\hat{n}_{i\downarrow}\left[B_1 Q_i + B_2 Q_i^2 + \cdots\right]$$

Centrosymmetric molecule, odd mode: A1=B1=0

→ Q^2 leads to effective displacement of U-term

$$U \to U + \delta U \left[1 - \cos 2\Omega_{ir} t\right]$$

Based on orbital-dependent modulation of U, a mechanism for light-enhanced SC in fullerenes has been proposed

PHYSICAL REVIEW B **94**, 155152 (2016)

Enhancing superconductivity in A_3C_{60} fullerides

Minjae Kim,[1,2,*] Yusuke Nomura,[1] Michel Ferrero,[1,2] Priyanka Seth,[2,3] Olivier Parcollet,[2,3] and Antoine Georges[1,2,4]

Non-equilibrium superconductivity in driven alkali-doped fullerides

Giacomo Mazza[1,2,*] and Antoine Georges[2,1,3]

arXiv:1702.04675

Other proposed explanations:
Millis et al.
Fabrizio et al.

Many other effects from Non-Linear Phononics…

- Ultra-fast switching of polarization in ferroelectrics
  (Theory: A.Subedi, Experiment: R.Mankowsky et al.)

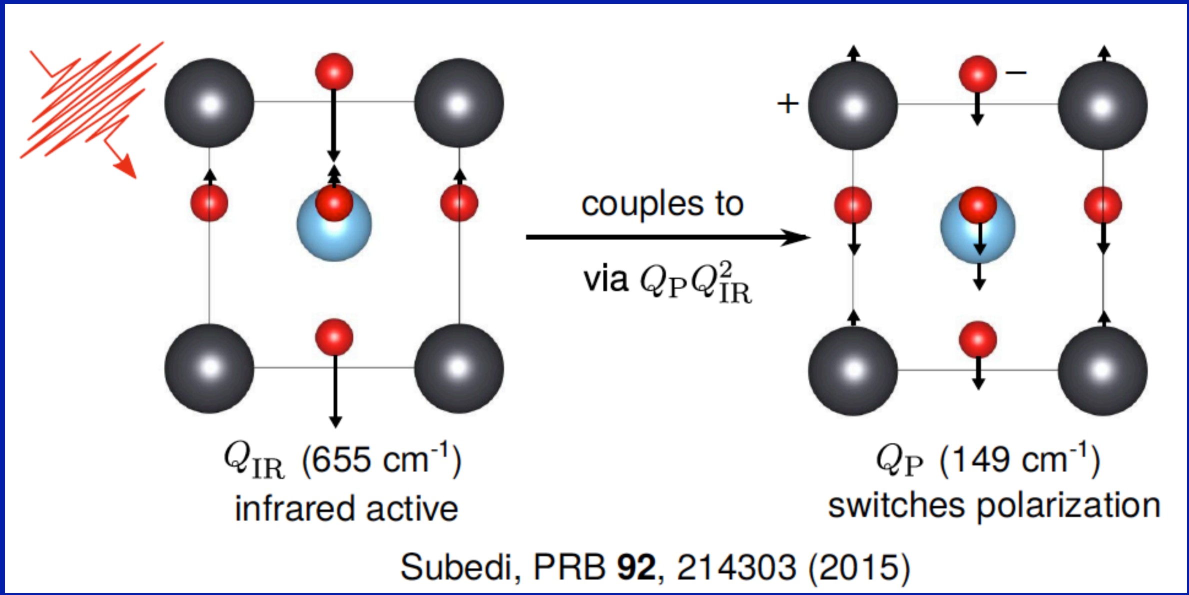

Courtesy: A.Subedi

- Acting on magnetism of Nickelates/STO by pumping STO
- More: see A.Cavalleri's lectures

Take-Home Message - Lecture 6: Selective Control of Quantum Materials by Resonant Light-Pulses

- Insulator-Metal transition
- Induced/Enhanced Superconductivity
- Non-Linear Phononics

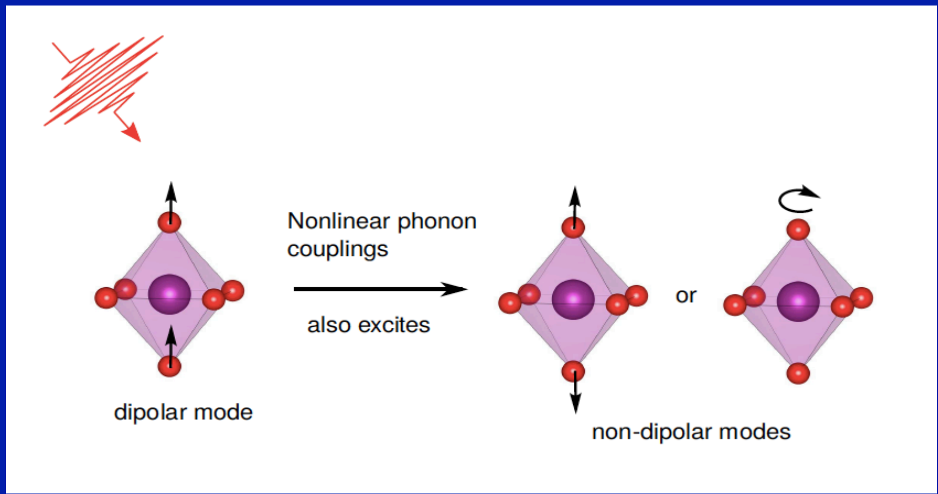

- Direct driving → modulation of U or hopping.

Take-Home message from these lectures: New routes to Control and Design of TMOs

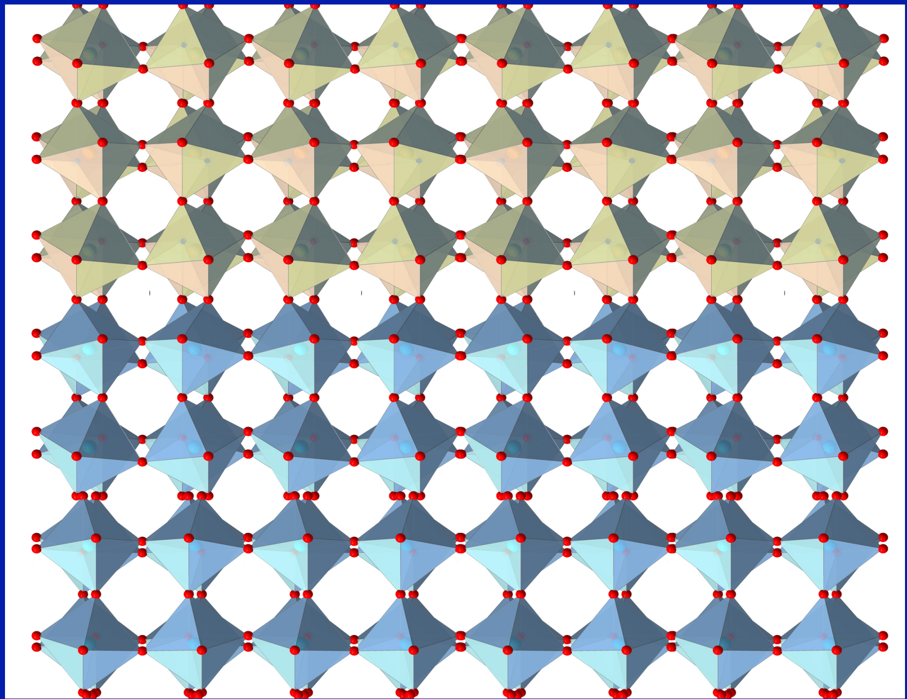

Artificial Materials:
Strained films and
Heterostructures
“Oxytronics/Mottronics”

Selective control with LIGHT

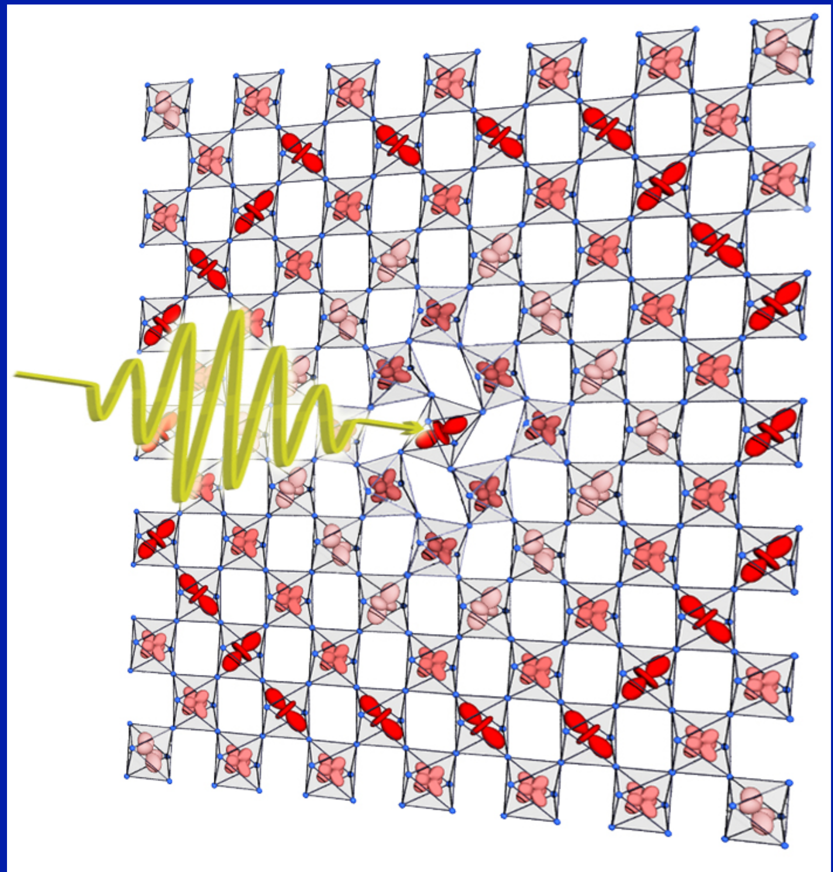

CONTROL: Traditional and Novel routes

Bandwidth	Pressure Size of rare-earth Distortion Tolerance factor 3d,4d,5d metal	Strained thin films and heterostructures Light/non-linear phononics
Crystal field, Orbital degeneracy	Size of rare-earth Distortion Tolerance factor	- Same -
Filling of shell	Chemistry	Ionic liquids Gating
Doping	Sr,Ca^{2+} → La, RE^{3+}	
Interaction strength	3d,4d,5d metal	Tunable dielectric gating ? Light ?
Charge-Transfer	Change apical oxygen distance Change ligand: O→ S, Se…	Light ?

This is the last lecture of this 2016-2017 cycle

BUT:

On Tue June, 13 at 10:00

We shall have a seminar

by Olle Eriksson

University of Uppsala

Data-mining approaches to find new materials

In this presentation I will introduce electronic structure theory, and describe how information calculated without input from experiments (so called ab-initio theory) can be used to find materials with potentially tailored properties. Examples will be given for potentially new superconductors, new two-dimensional materials as well as correlated electronic structures where the Kondo effects sets in. I will also outline how theory can be used to make a connection to an effective spin-Hamiltonian, for investigations of magnetization dynamics at time-scales down to sub-pico-seconds, and examples of simulations of all-thermal switching will be given.

Merci d’avoir assisté à ce cycle de cours !